LJMU Research Online

Towle, I, O'Hara, MC, Leece, AB, Herries, AIR, Adjei, A, Guatelli-Steinberg, D, Martínez de Pinillos, M, Modesto-Mata, M, Thiebaut, A, Hernando, R, Irish, JD, Guy, F, Boisserie, J-R and Hlusko, LJ

Uniform, circular, and shallow enamel pitting in hominins: Prevalence, morphological associations, and potential taxonomic significance

https://researchonline.ljmu.ac.uk/id/eprint/26536/

Article

Citation (please note it is advisable to refer to the publisher's version if you intend to cite from this work)

Towle, I, O'Hara, MC, Leece, AB, Herries, AIR, Adjei, A, Guatelli-Steinberg, D, Martínez de Pinillos, M, Modesto-Mata, M, Thiebaut, A, Hernando, R, Irish, JD, Guy, F, Boisserie, J-R and Hlusko, LJ (2025) Uniform, circular, and shallow enamel pitting in hominins: Prevalence, morphological

LJMU has developed **LJMU Research Online** for users to access the research output of the University more effectively. Copyright © and Moral Rights for the papers on this site are retained by the individual authors and/or other copyright owners. Users may download and/or print one copy of any article(s) in LJMU Research Online to facilitate their private study or for non-commercial research. You may not engage in further distribution of the material or use it for any profit-making activities or any commercial gain.

The version presented here may differ from the published version or from the version of the record. Please see the repository URL above for details on accessing the published version and note that access may require a subscription.

For more information please contact researchonline@ljmu.ac.uk

http://researchonline.ljmu.ac.uk/

Journal of Human Evolution 204 (2025) 103703

Contents lists available at ScienceDirect

Journal of Human Evolution

journal homepage: www.elsevier.com/locate/jhevol

Uniform, circular, and shallow enamel pitting in hominins: Prevalence, morphological associations, and potential taxonomic significance

Ian Towle [a, b, *], Mackie C. O'Hara [c], A.B. Leece [d, e], Andy I.R. Herries [d, f], Afua Adjei [d], Debbie Guatelli-Steinberg [g], Marina Martínez de Pinillos [b], Mario Modesto-Mata [b], Arthur Thiebaut [b], Raquel Hernando [b], Joel D. Irish [h, i], Franck Guy [j], Jean-Renaud Boisserie [j, k], Leslea J. Hlusko [b]

[a] Department of Anatomy and Developmental Biology, Biomedicine Discovery Institute, Monash University, Melbourne, Victoria, 3800, Australia
[b] Centro Nacional de Investigación sobre la Evolución Humana (CENIEH), Paseo Sierra de Atapuerca 3, 09002, Burgos, Spain
[c] School of Anthropology and Conservation, University of Kent, Canterbury, CT2 7NZ, UK
[d] Palaeoanthropology Lab, Department of Archaeology and History, La Trobe University, Bundoora, VIC, 3086, Australia
[e] Geoarchaeology and Archaeometry Research Group, Southern Cross Geoscience, Southern Cross University, Lismore, NSW, 2480, Australia
[f] Palaeo-Research Institute, University of Johannesburg, Gauteng, 2092, South Africa
[g] Department of Anthropology, The Ohio State University, 174 West 18th Ave, Columbus, OH, 43210, USA
[h] School of Biological and Environmental Sciences, Liverpool John Moores University, Liverpool L3 3AF, UK
[i] Centre for the Exploration of the Deep Human Journey, University of the Witwatersrand, Private Bag 3, WITS 2050, South Africa
[j] Laboratory Paleontology Evolution Paleoecosystems Paleoprimatology (PALEVOPRIM), CNRS & Université de Poitiers, Poitiers, F-86000 France
[k] French Centre for Ethiopian Studies (CFEE), CNRS & Ministry of Europe and Foreign Affairs, PO Box 5554 Addis Ababa, Ethiopia

ARTICLE INFO

Article history:
Received 28 November 2024
Accepted 13 May 2025
Available online xxx

Keywords:
Pitting enamel hypoplasia
Paranthropus
Australopithecus
Hominin taxonomy

ABSTRACT

This study explores a particular form of enamel pitting originally identified in *Paranthropus robustus*. We call this uniform, circular, and shallow (UCS) pitting to distinguish it from more irregular and nonuniform defects often associated with enamel hypoplasia. We pose the hypothesis that UCS pitting is unique to the genus *Paranthropus*. We test this by investigating hominin dental remains from the ca. 3.4 Ma to ca. 1.1 Ma fossiliferous sequence at Omo, Ethiopia ($n = 76$) to look for evidence of UCS pitting in an assemblage that includes at least three hominin genera (*Australopithecus*, *Paranthropus*, and *Homo*). We also examine the correlation between UCS pitting, tooth size, enamel thickness, and cusp proportions in samples from both eastern Africa (Omo) and southern Africa (Drimolen Main Quarry ~2.04–1.95 Ma, Swartkrans ~1.9–1.4 Ma, and Kromdraai ~1.95–1.78 Ma). In the Omo specimens, we found UCS pitting similar to that seen in *P. robustus*. While we observed this pitting on five of 24 permanent teeth and two deciduous molars from both *Paranthropus aethiopicus* and *Paranthropus boisei*, we also identified UCS pitting on five of 13 non-*Paranthropus* hominin permanent posterior teeth from Member B (~3.0 Ma). Our correlation studies yielded no association between the presence of UCS pitting and variation in tooth size, enamel thickness, or cusp proportions. The consistent appearance and characteristics of UCS pitting suggest a shared etiology. Our findings also suggest that UCS pitting may result from a genetic effect related to enamel formation, potentially in association with specific environmental or dietary factors.
© 2025 The Author(s). Published by Elsevier Ltd. This is an open access article under the CC BY license (http://creativecommons.org/licenses/by/4.0/).

1. Introduction

Enamel defects are typically classified based on the stage of enamel formation in which they occur—either during the secretory or maturation phase (Ten Cate, 1994; Guatelli-Steinberg, 2015; Xing et al., 2016). Enamel hypoplasia occurs during the secretory stage of enamel formation. In studies of primate fossils, enamel hypoplasia is frequently observed and reported, presenting in various forms (e.g., Tobias, 1967; Lukacs, 2001a,b; Guatelli-Steinberg et al., 2004; Xing et al., 2016; Towle and Irish, 2020). Enamel hypoplasia is often divided into four main categories: localized-, linear-, pit-, and plane-form hypoplasia (Pindborg, 1970; Seow, 1990; Towle et al., 2017; Skinner, 2023). Despite their varied appearances, these defects all stem from a reduction in enamel matrix, a consequence of

* Corresponding author.
E-mail address: ianetowle@gmail.com (I. Towle).

https://doi.org/10.1016/j.jhevol.2025.103703
0047-2484/© 2025 The Author(s). Published by Elsevier Ltd. This is an open access article under the CC BY license (http://creativecommons.org/licenses/by/4.0/).

disruptions during ameloblast production (Eversole, 1984). Categorizing defects into one of these four types can be challenging (e.g., Ogden et al., 2007). The etiology of enamel hypoplasia ranges from injuries to the tooth during development to diseases or malnutrition that impacts tooth formation; similar defects can also be associated with specific genetic conditions, including amelogenesis imperfecta (AI) (Collins Cook, 1980; Goodman and Rose, 1991; Skinner and Newell, 2003; Smith et al., 2017). Hence, studying enamel defects can reveal insights into diets, genetics, environmental factors, and the overall health of individuals and populations (e.g., Cunha et al., 2004; Ogden et al., 2007; Smith et al., 2017; O'Hara et al., 2023).

The methods used for recording enamel defects vary substantially across studies. Some researchers limit their observations to specific teeth, often excluding postcanine and deciduous teeth (e.g., Infante and Gillespie, 1974; Lovell and Whyte, 1999). Many focus on the frequency of linear enamel hypoplasia (LEH) (e.g., Guatelli-Steinberg et al., 2004; Miszkiewicz, 2015; Nakayama, 2016), while others consider all types of defects, whether they are linear or not (e.g., Goodman et al., 1980; Ogilvie et al., 1989; Towle and Irish, 2020). Pitting enamel hypoplasia (PEH) also varies substantially as it can be localized or similar to the plane-form type of defect and is sometimes recorded as part of LEH bands (Sognnaes, 1956; Goodman et al., 1980, 1984; Hillson, 1992; Hillson and Bond, 1997). Pitting enamel hypoplasia presents as circular pinpricks to larger irregular depressions on the enamel surface (Skinner, 1996; Hillson and Bond, 1997; Witzel et al., 2006; Ogden et al., 2007; Towle and Irish, 2019), with varying distributions across the tooth crown. The depth and location of these pits can provide clues about the timing and etiology of the defects (Hillson and Bond, 1997). However, the factors leading to the formation of PEH, as opposed to other hypoplasia types like LEH, are still being explored, with considerations given to tooth type, crown position, and the cause of disruption.

In this study, we investigate a specific type of enamel pitting observed in *Paranthropus robustus* (Towle and Irish, 2019). The etiology of this pitting is at present unknown; we (Towle and Irish, 2019) have previously suggested that it may not constitute the 'defects' typically associated with physiological stress during development but may have directly resulted from unique enamel formation processes (Towle and Irish, 2019). Considering the diverse types of enamel pitting documented in hominins and other primates, we introduce new terminology in this study. We define this form of pitting in *P. robustus* as uniform, circular, and shallow (UCS) pitting, setting it apart from many other types of defects that have been considered PEH. Indeed, examples considered to be enamel pitting defects vary widely in size and shape, suggesting a broad spectrum of etiologies.

At present, UCS pitting—defined by multiple shallow circular pits clustering on the enamel surface and not associated with linear-/horizontal-type features (e.g., not forming 'bands')—has only been commonly found on deciduous and permanent postcanine teeth of *P. robustus* (Fig. 1). Uniform, circular, and shallow pitting can cover the whole crown, but in some cases, clusters of UCS pitting are visible only on particular surfaces. The precise cause of UCS pitting in *P. robustus*—whether it relates to conditions like AI, pleiotropic effects, and normal variation in enamel formation or to a specific environmental factor—remains uncertain. However, Towle and Irish (2019) proposed that UCS pitting may be associated with the evolution of hyperthick enamel characteristic of *Paranthropus* megadontia. If so, and if *Paranthropus* is a monophyletic taxon, then *Paranthropus aethiopicus* and *Paranthropus boisei* should be expected to also display UCS pitting. We therefore hypothesize in the present study that this pitting is (1) unique to the genus *Paranthropus* and present in both eastern and southern African species and (2) correlated with features associated with megadontia (larger tooth sizes, thicker enamel, and variation in cusp proportions).

2. Materials and methods

2.1. Materials

Our test of the two hypotheses was conducted on a sample of hominin fossils that includes specimens from eastern and southern Africa. The first hypothesis is tested using the eastern African sample that derives from the Omo Group deposits from Ethiopia, a sedimentological sequence that encompasses 2.3 Myr of hominin evolution and preserves evidence of three genera: *Australopithecus*, *Homo*, and *Paranthropus*. The second hypothesis is tested with data

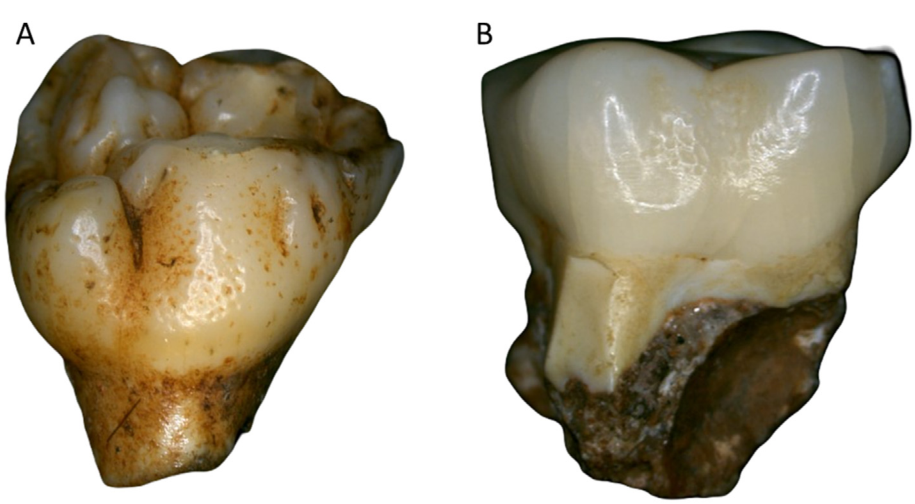

Figure 1. Uniform, circular, and shallow pitting on two *Paranthropus robustus* teeth from Drimolen Main Quarry (DMQ; southern Africa). A) DNH 36 (upper second deciduous molar), distal. Uniform, circular, and shallow pitting is seen on the lingual surface facing forward. This appears as small indentations that are regularly distributed across the enamel surface. B) DNH 30, lingual (upper second deciduous molar). Uniform, circular, and shallow pitting is seen between the mesial and distal cusps as dimpling, with small indentations that are regularly spaced. Scale bar: 10 mm. (For interpretation of the references to color in this figure, the reader is referred to the web version of this article.)

from the Omo sample, as well as southern African specimens of *Paranthropus*, as described in detail in the following paragraphs. The data that support the findings of this study are available in the Results section and Supplementary Online Material [SOM] of this article. The data are also available through Dryad (Towle et al., 2025).

Eastern Africa: the Omo sample The combined sequences of the Shungura Formation and Usno Formation offer a unique opportunity to look at UCS pitting occurrence through time in the hominin lineage, with samples from ca. 3.4 Ma to ca. 1.1 Ma (Howell and Coppens, 1976; Boisserie et al., 2008; Hlusko et al., 2024). A total of 71 permanent postcanine Omo teeth were studied (molars and premolars) from collections made by the International Omo Research Expedition (IORE, 1967–1976) and Omo Group Research Expedition (OGRE, since 2006). These specimens are mostly isolated teeth, but a few are associated teeth or jaw fragments with multiple teeth. While many IORE specimens were previously assigned to taxa (Arambourg and Coppens, 1968; Howell and Coppens, 1976; Suwa et al., 1996; Boisserie et al., 2008; Bobe and Leakey, 2009; Wood and Leakey, 2011), an updated, larger taxonomic study that includes both the IORE and the OGRE collections—maxillary as well as mandibular isolated teeth—provides the taxonomic framework followed here (Hlusko et al., 2024). An additional, small set of isolated anterior teeth are also present in the Omo sequences, but are not included in the present study.

The list of Omo specimens in our analysis and the taxonomic assignment of each are listed in Table 1, following Hlusko et al. (2024), with five deciduous teeth added following the classification described earlier. In a previous taxonomic study, Suwa et al. (1996) divided the Omo sample into 'robust' and 'nonrobust' categories. Since then, new discoveries have revealed evidence of a megadont non-*Paranthropus* species, *Australopithecus garhi* (Asfaw et al., 1999). Consequently, the term 'robust' may not necessarily be as useful of a term to separate species of *Paranthropus* and *Australopithecus*. Therefore, an informal taxonomic category was developed to include all Late Pliocene representatives of *Australopithecus* (*Australopithecus* LP; Hlusko et al., 2024). In their analysis of a large sample of comparative hominin teeth, Hlusko et al. (2024) also found considerable morphological and size overlap between *Australopithecus* LP and early specimens of the genus *Homo* from eastern Africa (*Homo* early eastern Africa, abbreviated as *Homo* EEA). Therefore, many isolated teeth can only be assigned to the combined informal taxonomic category *Australopithecus* LP/*Homo* EEA (Hlusko et al., 2024).

Five deciduous teeth from the IORE hominin collections show UCS pitting: L 64-2, L 704-2, OMO 222-1973-2744 (two teeth), and L 144-23. Given the size of L 64-2 and L 704-2, these have both long been attributed to a species now within the paradigm of *Paranthropus* (Howell, 1969; Howell and Coppens, 1973). In contrast, L 144-23 has been interpreted as more 'nonrobust' (Howell and Coppens, 1973) and OMO 222-1973-2744 has similarities to specimens of early *Homo* (Condemi, 2004). These teeth are part of a current taxonomic study of the deciduous dentition by the OGRE project, but we mention them here and show them in Figures 3 and 5 to demonstrate that UCS pitting is present in deciduous teeth from eastern Africa as well as the southern African assemblages mentioned previously.

2.2. Southern African samples of Paranthropus

In addition to the Omo (eastern Africa) sample, we also studied a southern African subsample from Drimolen Main Quarry (DMQ; southern Africa), Swartkrans (southern Africa), and Kromdraai (southern Africa) (Table 2; SOM Tables 1 and 2). The Swartkrans samples come from Member 1 Hanging Remnant and Member 2, which date between 1.9 and ~1.4 Ma (Herries, 2022). The DMQ sample dates between 2.04 and 1.95 Ma (Herries et al., 2020; Martin et al., 2021). The Kromdraai sample is poorly dated, but preliminary paleomagnetic analysis suggests it is between 1.95 and 1.78 Ma (Thackeray et al., 2002; Herries, 2022). Overall, the southern African sample ranges between ~2.04 and ~1.4 Ma (Herries, 2022). They include material suggested to represent two separate 'temporal subspecies' within *P. robustus*: *Paranthropus robustus robustus* (Swartkrans and Kromdraai) and *Paranthropus robustus ukusa* (DMQ) (Martin et al., 2024).

2.3. Data collection

We recorded the presence/absence of UCS pitting in the Omo samples, preserved at the Ethiopian Heritage Authority (Addis Ababa). We also collected data to assess potential associations between tooth size, enamel thickness, and cusp proportions with UCS pitting. One specimen from each fossil assemblage was also assessed for UCS pit depth and diameter. The methodology for each type of analysis is described below. Visualization of data (Figs. 6–9) was performed in Python programming language, utilizing the following libraries: Pandas (data handling), Scikit-learn (principal component analysis [PCA] implementation), and Seaborn/Matplotlib (figure creation).

Assessment of uniform, circular, and shallow pitting The presence and characterization of enamel pitting was recorded following the assessment of original fossils, casts, high-resolution images from multiple perspectives, images captured using a Dino-Lite AF3113T digital microscope (AnMo Electronics Corporation, New Taipei City, Taiwan), and μCT scans. Specimens with substantial postmortem damage were not included. The classification of enamel pitting follows Towle and Irish (2019, 2020) for PEH to differentiate postmortem effects and other causes. All identified enamel pitting in the Omo assemblage is consistent with the definition of UCS pitting, and therefore, we use this term exclusively in the rest of this manuscript. To determine the presence/absence of UCS pitting, data for specific Swartkrans, DMQ, and Kromdraai specimens were collected using the same methods as applied to the Omo assemblage.

Tooth linear measurements For this analysis, we focus on upper first molars in a single species, *P. robustus*, from both Swartkrans and DMQ. Mesiodistal (MD) and buccolingual (BL) linear distances were taken following standard procedures (Wood et al., 1983; Wood and Xu, 1991). We first conducted a univariate statistical analysis (in Microsoft Excel) to obtain mean and SD. A scatterplot and kernel density estimation (KDE) display the result of the measurements, with the specimens categorized based on the presence or absence of UCS pitting. The KDE plot displays the distribution of each measurement within each enamel pitting category. Specimens used in these analyses, and the associated MD and BL measurements for each, are listed in SOM Table S1.

Enamel thickness We also investigated the association between UCS pitting and relative enamel thickness (RET) in upper and lower first and second molars, again focusing on *P. robustus*. The dataset comprised measurements from a total of 31 *P. robustus* specimens, each classified for UCS pitting and tooth type, alongside their corresponding RET values. Thirty RET values were collected from O'Hara (2021), and an additional specimen was measured for the present study (DMQ specimen DNH 108a). All measurements were

Table 1
Omo specimens studied for enamel pitting, taxonomy (from Hlusko et al., 2024), and UCS pitting status.

Specimen number	Dental elements	Stratigraphic level	Taxonomic group	UCS pitting
B 8-14B	lt P4	Usno (equivalent to Shungura Member B)	*Australopithecus* LP	No
B 8-23 a	lt P4	Usno (=B)	*Australopithecus* LP	No
B 8-23 b	lt M1	Usno (=B)	*Australopithecus* LP	No
L 1/nn-10010a	rt m2	B	*Australopithecus* LP/*Homo* EEA	Yes
L 1/nn-10010b	lt m2	B	*Australopithecus* LP/*Homo* EEA	Yes
L 2-89	lt m3	B	*Australopithecus* LP/*Homo* EEA	Yes
L 795-1	rt m3	B	*Paranthropus*	Yes
OMO 28/S-1968-30	rt m3	B	*Paranthropus*	No
OMO 112/2-10029b	rt M3	B	*Australopithecus* LP/*Homo* EEA	Yes
OMO 112/4-10009	lt P3	B	*Australopithecus* LP	Yes
W 7-23	lt p4	Usno (=B)	*Australopithecus* LP	No
W 7-508	rt m1	Usno (=B)	*Australopithecus* LP/*Homo* EEA	No
W 8-749	rt M1	Usno (=B)	*Australopithecus* LP	No
W 8-752	rt m1	Usno (=B)	*Australopithecus* LP/*Homo* EEA	No
W 8-988	lt P4	Usno (=B)	*Australopithecus* LP	No
L 45-2	rt m1	C	*Australopithecus* LP/*Homo* EEA	No
L 51-1	lt m1	C	*Australopithecus* LP/*Homo* EEA	No
L 51-2	lt M1	C	*Australopithecus* LP/*Homo* EEA	No
L 51-3	lt M2	C	*Australopithecus* LP/*Homo* EEA	No
L 51-4	lt M1	C	*Australopithecus* LP/*Homo* EEA	No
L 51-79	rt p4	C	*Paranthropus*	No
L 51-80	rt p4	C	*Australopithecus* LP/*Homo* EEA	No
L 51-10002	rt m3	C	*Australopithecus* LP/*Homo* EEA	No
L 62-17	rt m2	C	*Paranthropus*	No
OMO 18-1968-31	lt p3	C	*Paranthropus*	No
OMO 18-1968-33	lt p3	C	*Australopithecus* LP/*Homo* EEA	No
OMO 18-1968-34	lt m1	C	*Paranthropus*	No
OMO 18-1970-1799	lt M2	C	*Paranthropus*	Yes
OMO 69-1974-900	lt P4	C	*Australopithecus* LP/*Homo* EEA	No
OMO 84-10001	lt M1	Uncertain member	cf. *Homo*	No
OMO 157-10009a	lt m3	C	*Australopithecus* LP/*Homo* EEA	No
OMO 224-10005	rt m2	C	*Australopithecus* LP/*Homo* EEA	No
OMO 329-10015	rt m3 germ	C	*Australopithecus* LP/*Homo* EEA	No
OMO 349-10003	lt m2	C	*Australopithecus* LP/*Homo* EEA	No
L 144-23	lt dM2	C	*Australopithecus* LP/*Homo* EEA[a]	Yes
L 50-2	lt M2	D	*Paranthropus*	No
L 824-5	lt m1	D	*Australopithecus* LP/*Homo* EEA	No
L 64-2	lt dm2	D	*Paranthropus*[a]	Yes
L 704-2	lt dm1	D	*Paranthropus*[a]	Yes
L 26-1G	rt m1	E	*Australopithecus* LP/*Homo* EEA	Yes
L 338/X-34	lt M2	E	*Paranthropus*	No
L 338/X-35	rt P3	E	*Paranthropus*	No
L 338/X-39	lt m3	E	*Paranthropus*	No
L 338/X-40	lt p4	E	*Paranthropus*	No
L 28-30	rt m3	F	cf. *Homo*	No
L 28-58	rt M1	F	*Homo*	No
L 157-35	lt m2	F	*Paranthropus*	No
L 238-35	rt M2	F	cf. *Australopithecus garhi*	No
L 398-120	rt p3	F	*Paranthropus*	No
L 398-573	lt M3	F	*Australopithecus* LP/*Homo* EEA	No
L 398-630	rt m3	F	*Paranthropus*	Yes
OMO 33-1969-9	Rt m3	F	*Paranthropus*	No
OMO 33-1970-63	rt M3	F	*Australopithecus* LP/*Homo* EEA	No
OMO 33-1971-507	P4 frag	F	*Paranthropus*	Yes
OMO 33-1971-508	rt p4	F	*Paranthropus*	No
OMO 33-1973-3282	lt P4	F	*Australopithecus* LP/*Homo* EEA	No
OMO 33-1973-5496	lt p3	F	*Australopithecus* LP/*Homo* EEA	No
OMO 123/N-1973-5495	rt p3	F	cf. *Homo*	No
OMO 174-10002	lt m3	F	*Homo*	No
L 7-279	lt m2	G	*Homo*	No
L 628-1	lt p4	G	*Paranthropus*	No
L 628-3	lt m3	G	*Paranthropus*	Yes
L 628-4	lt p4	G	cf. *Paranthropus*	No
L 628-9	lt m1	G	*Paranthropus*	No
L 628-10	lt m2	G	cf. *Paranthropus*	No
OMO Sh 1/1-1969-17	lt M1	G	*Homo*	No
OMO 29/1-1968-43	rt p3	G	cf. *Homo*	No
OMO 47-1968-46	rt m2	G	*Paranthropus*	No
OMO 75/S-1969-15	lt m1	G	cf. *Homo*	No
OMO 222-1973-2744	Lt dm1 and dm2	G	cf. *Homo*[a]	Yes

Table 1 (*continued*)

Specimen number	Dental elements	Stratigraphic level	Taxonomic group	UCS pitting
OMO VE 3-10011	lt m3	H	*Homo*	No
OMO K 7-1969-19	lt m2	L	cf. *Homo*	No
OMO 383-10124 a	lt M1	L	*Homo erectus*	No
OMO 383-10124 b	lt M2	L	*Homo erectus*	No
OMO 389-10085	rt m3	L	*Homo erectus*	No

P = premolar; M = molar (capital signifies a maxillary element and lowercase mandible); *Australopithecus* LP = Late Pliocene representatives of *Australopithecus*; *Homo* EEA = early specimens of the genus *Homo* from eastern Africa. The five deciduous teeth begin with a 'd' in the Dental elements column.
[a] Species classifications based on published descriptions (Howell, 1969; Howell and Coppens, 1973; Condemi, 2004).

taken using standardized methodology from μCT scans (Skinner et al., 2015; Lockey et al., 2020; O'Hara, 2021). A descriptive statistical analysis was conducted in Microsoft Excel to summarize the distribution of RET across different categories (i.e., tooth type and UCS pitting). Additionally, the data were visualized using box and whisker plots (Python, Seaborn/Matplotlib) to illustrate the distribution of RET across different tooth types and UCS pitting status.

Table 2
Samples studied from the South African sites of Drimolen, Swartkrans, and Kromdraai.

Specimen	Tooth	Site	UCS pitting
DNH 106	UM1	Drimolen	No
DNH 14	UM1	Drimolen	No
DNH 152d	UM1	Drimolen	Yes
DNH 155	UM1	Drimolen	No
DNH 4	UM1	Drimolen	Yes
DNH 60B	LM1	Drimolen	No
DNH 60C	LM2	Drimolen	No
DNH 84B	UM1	Drimolen	Yes
DNH 108A	UM1	Drimolen	Yes
DNH 57B	UM1	Drimolen	No
DNH 60	UM1	Drimolen	No
SK (826B) 828	LM1	Swartkrans	No
SK 1	LM2	Swartkrans	No
SK 102	UM1	Swartkrans	Yes
SK 13	UM1	Swartkrans	No
SK 13.14	UM2	Swartkrans	No
SK 14129A	UM1	Swartkrans	No
SK 1587A	LM2	Swartkrans	No
SK 1591	UM1	Swartkrans	No
SK 17	UM1	Swartkrans	No
SK 25	LM2	Swartkrans	Yes
SK 3974	LM1	Swartkrans	No
SK 47	UM1	Swartkrans	No
SK 47	UM2	Swartkrans	No
SK 48	UM2	Swartkrans	No
SK 49	UM2	Swartkrans	Yes
SK 52	UM1	Swartkrans	No
SK 55A	UM1	Swartkrans	No
SK 6	LM1	Swartkrans	No
SK 6	LM2	Swartkrans	No
SK 61	LM1	Swartkrans	Yes
SK 62	LM1	Swartkrans	No
SK 63	LM1	Swartkrans	Yes
SK 826A	UM2	Swartkrans	No
SK 832	UM1	Swartkrans	No
SK 838A	UM1	Swartkrans	Yes
SK 843.846A	LM2	Swartkrans	No
SK 872	UM1	Swartkrans	No
SKW 5	LM2	Swartkrans	No
SKX 4446	LM2	Swartkrans	No
TM 1517A	UM2	Kromdraai	Yes
TM 1601	UM1	Kromdraai	No
KB 5223	LM1	Kromdraai	No

All samples are considered to belong to *Paranthropus robustus*.

The specimens studied, and their respective RET values, are listed in SOM Table S2.

Cusp area analysis Cusp area data are from Hlusko et al. (2024) for a total of nine lower third molars from Omo. Occlusal images of complete molars were analyzed using ImageJ software (Schindelin et al., 2015), with outlines of each cusp following the methodology of Wood et al. (1983) but with the updated methods of using ImageJ following Brophy et al. (2021) and Bailey et al. (2004). Total crown area was also calculated by summing all cusps (following Wood et al., 1983). The dataset comprised measurements of different lower molar cusps commonly found in fossil hominins: protoconid, metaconid, hypoconid, entoconid, hypoconulid, entoconulid (cusp 6), and metaconulid (cusp 7), which were transformed into ratios to focus on relative, rather than absolute size differences. A PCA was performed (Python, Scikit-learn library) to explore if teeth with UCS pitting form a cluster/grouping. Cusp size values for each specimen are listed in SOM Table S3.

Pit diameter analysis The diameter was measured for 10 pits per tooth on 11 specimens from Omo and DMQ. The diameter of pits was assessed using two methods, based on either scaled images (following the protocol of the cusp area analysis) or μCT scans (following the methodology of Towle and Irish, 2019). In each case, 10 pits clearly visible macroscopically were recorded from a total of 11 specimens from Omo and DMQ (SOM Table S4); an additional six specimens were added for Swartkrans using data from Towle and Irish (2019). Two specimens from the same individual were also assessed to assess variation between tooth types in the same individual (OMO 222-1973-2744; dm1 and dm2).

Pit depth analysis We measured the depth of six pits on three teeth for a total of 18 pits (SK 64, DNH 30, and L 1/nn-10010a; Swartkrans, Drimolen, and Omo, respectively). Pit depth was assessed using μCT scans for a single specimen at each site (Omo, Swartkrans, and DMQ). Specimens were selected based on perceived severity of the pitting (macroscopically), with SK 64 (Swartkrans) having very defined UCS pitting, through DNH 30 (DMQ), to L 1/nn-10010a (Omo), in which the UCS pitting appears fainter (SOM Table S5). The analysis was performed in Fiji (version 2.9.0), where scans were scaled using the known isometric voxel size with the 'Set Scale' function. Specimens were oriented with the occlusal surface directly up, with a BL slice that optimizes the deepest point of each pit. Then the Straight-Line tool was used to measure depth, from the deepest point to approximately where the enamel would have ended if there was no pit (i.e., tracing a line from the adjacent 'normal' enamel). The thickness of enamel underneath the pit was then measured as the shortest distance from the pit bottom to the enamel-dentine junction (EDJ; Fig. 2). Each pit depth was then divided by the total thickness (× 100) to get the percentage of the enamel thickness that each pit penetrates.

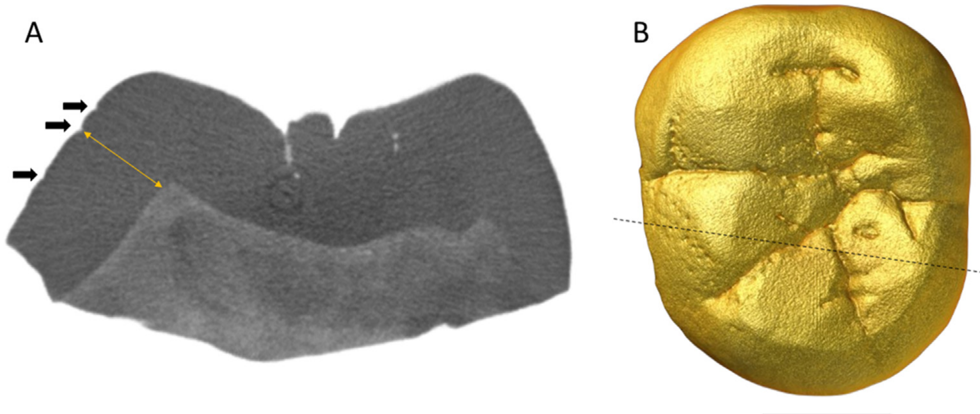

Figure 2. Omo specimen L 1/nn-10010a, showing A) a slice from buccal-lingual showing the depth of individual pits, and how enamel thickness under a pit was calculated (orange arrow); B) a surface rendering from the same μCT scan, highlighting the location of the slice in (A) with a dotted line. Scale bar: 5 mm. (For interpretation of the references to color in this figure, the reader is referred to the web version of this article.)

3. Results

Our results show UCS pitting is relatively common in the postcanine teeth of the Omo hominins (Fig. 3), although its presence is not evenly distributed across the stratigraphic levels, nor among the different taxa represented. Five permanent teeth of *Paranthropus* (five of 24) show UCS pitting (Fig. 4), spanning 2.97 Ma to 2.11 Ma, members C to G. In the earliest deposits (Usno Formation and Member B, from ~3.3 Ma to ~2.95 Ma), specimens attributed to Late Pliocene *Australopithecus* also show UCS pitting (five of 13 permanent postcanine teeth; Fig. 5). Specimens from the younger levels assigned to non-*Paranthropus* hominins (including *Homo* EEA and *Homo erectus*) do not show UCS pitting, with the possible exception of L 26-1G (taxonomic attribution: *Australopithecus* LP/*Homo* EEA, Suwa et al., 1996; Suwa et al., 2007; Wood and Leakey, 2011; Louail and Prat, 2018; Grine et al., 2019; Hlusko et al., 2024). However, this specimen often falls outside the range of comparative samples in different analyses and has been identified as either a lower first or second molar, complicating interpretations and comparisons (Hunt and Vitzthum, 1986; Howell et al., 1987; Suwa et al., 1996; Hlusko, 2004; Wood and Leakey, 2011; Skinner et al., 2015; Louail and Prat, 2018; Hlusko et al., 2024). The two deciduous molars previously described as belonging to a non-*Paranthropus* taxon/group (OMO 222-1973-2744; L 144-23; Table 1; Howell and Coppens, 1973; Condemi, 2004) also show UCS pitting.

Uniform, circular, and shallow pitting sometimes covers entire crowns and in other cases tends to cluster only on specific tooth surfaces. In some instances, occlusal wear may pose challenges in distinguishing small clusters of UCS pitting from other types of enamel defects. For example, in the L 2-89 specimen, despite the wear, UCS pitting is still discernible in at least two locations (Fig. 5). Similarly, in the L 704-2 specimen, although slightly worn, the

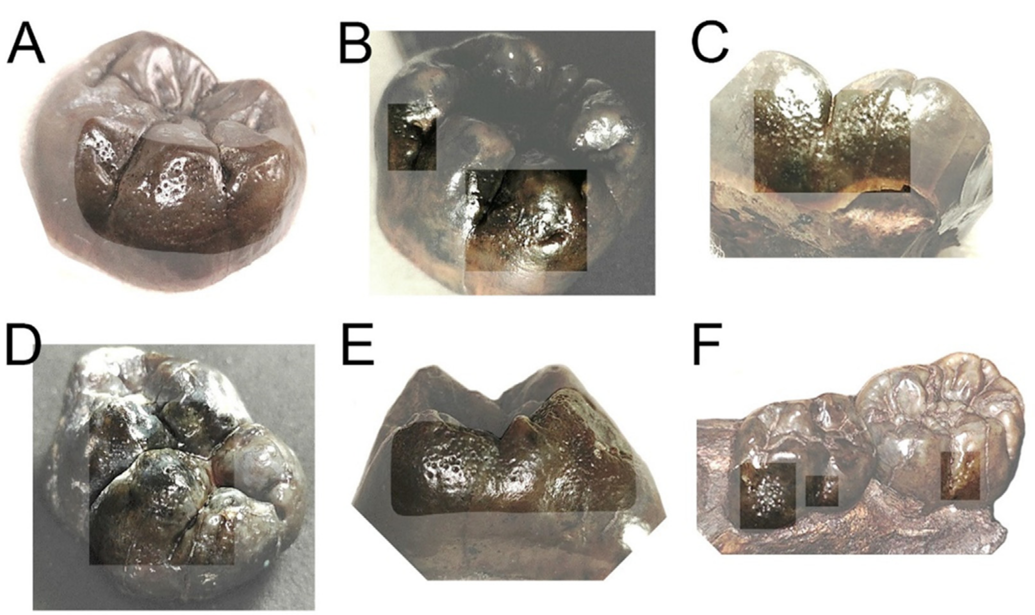

Figure 3. Composite figure of six specimens displaying uniform, circular, and shallow pitting, using a microscopic camera (Dino-Lite AF3113T): A) L 1/nn-10010a; B) L 26-1g; C) L 64-2; D) L 704-2; E) OMO 18-1799; F) OMO 222-2744. (For interpretation of the references to color in this figure, the reader is referred to the web version of this article.)

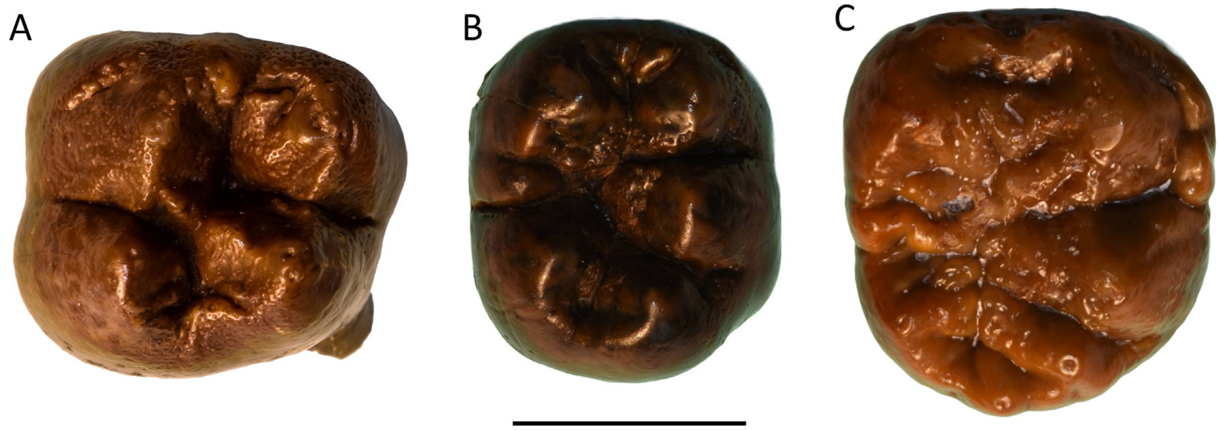

Figure 4. *Paranthropus* enamel pitting: A) OMO 18-1970-1799 (left upper second molar); B) L 26-1G (right lower first molar; shown from a different angle in Fig. 3); C) L 795-1 (lower right third molar). Scale bar: 10 mm. Shallow and circular enamel pitting can be clearly seen on the occlusal surface in all three examples, with other surfaces also affected to varying degrees. Note: L 26-1G is at present not confidently classified as *Paranthropus* and does not confirm confidently to any group; see text for details. (For interpretation of the references to color in this figure, the reader is referred to the web version of this article.)

crown seems to exhibit UCS pitting that may have previously covered more of the crown (Fig. 3D). Additionally, pitting visibility is often greatest on the occlusal surface where fissures and crenulations complicate identification, as seen in L 795-1 (Fig. 4C). Despite the complexity on the occlusal surface of L 795-1, the presence of shallow pitting on the buccal surface suggests classifying this as UCS pitting. These observations highlight potential slight variability in the appearance of UCS pitting in relation to wear and tooth morphology.

There is no evidence in our sample that variation in tooth size, cusp proportions, or enamel thickness correlates with the presence of UCS pitting. The MD vs. BL scatterplot and KDE show no distinct clustering or segregation between specimens with and without UCS pitting; this suggests that tooth size does not influence enamel pitting, and vice versa, as measured by MD and BL dimensions (Figs. 6 and 7). The mean RET for specimens with UCS pitting (28.93) was slightly higher than for those without (27.11). But as the box and whisker plot shows (Fig. 8), the variance in RET is similar for samples with and without UCS pitting for the maxillary and mandibular first molars that have the largest sample sizes. The PCA involving each individual cusp ratio also fails to distinguish between teeth with and without UCS pitting (Fig. 9). We also found no evidence that UCS pitting is associated with variation in occlusal area in the Omo samples as pitting is found in the largest and the smallest specimens (Table 3). Pit depth is relatively shallow (Fig. 2), especially when the thickness of enamel in these specimens was considered. From a specimen in which the pits look very defined, SK 64, the average pit depth is 16.1% of the enamel thickness. Two other specimens show more moderate (less defined) pitting, with equivalent depth values of 5.9% (DNH 30) and 5.2% (L 1/nn-10010a). The diameter of the pits is also small and consistent across sites and tooth types (Table 4). We also see that the variation in pit diameter on the same tooth is similar to the variation within the study sample (Table 4).

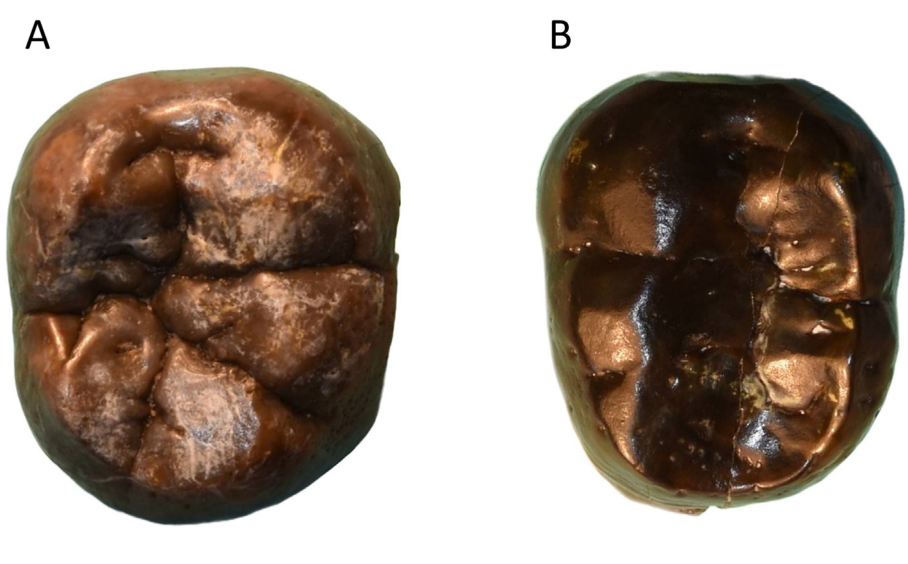

Figure 5. Omo nonrobust pitting: A) L 1/nn-10010a (lower right second molar; shown from a different angle in Fig. 3); B) L 2-89 (lower left third molar). Scale bar: 10 mm. Uniform shallow enamel pitting is visible on multiple surfaces in both cases. The pitting is faint, likely at least partly due to tooth wear reducing the pit depth through time. (For interpretation of the references to color in this figure, the reader is referred to the web version of this article.)

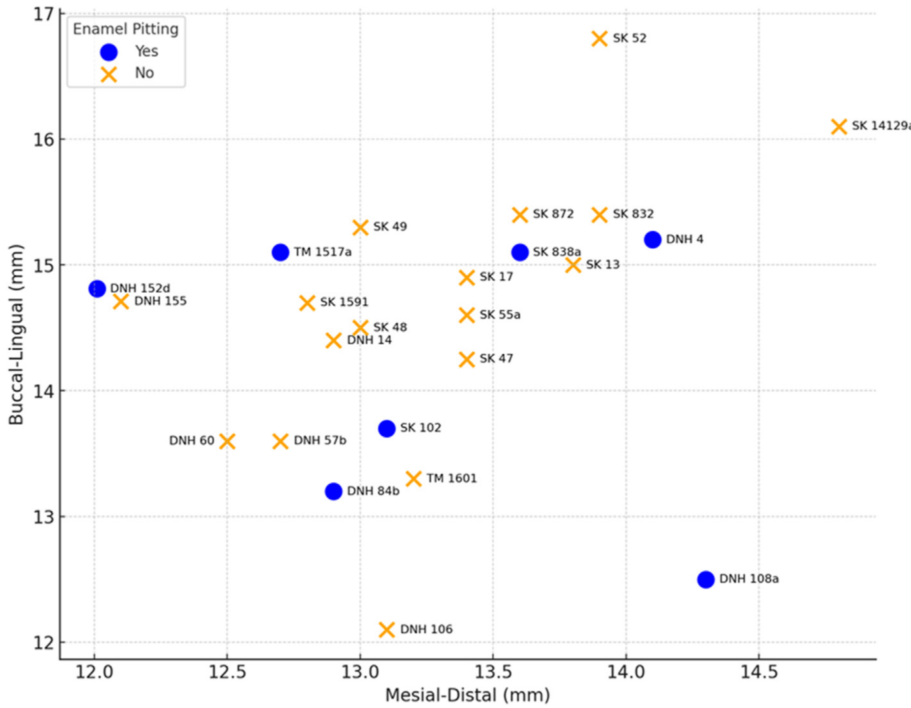

Figure 6. Scatterplot of tooth buccal-lingual and mesial-distal measurements split by teeth with and without uniform, circular, and shallow pitting. All samples are upper first molars belonging to *Paranthropus robustus*, from Swartkrans, Drimolen Main Quarry, and Kromdraai. (For interpretation of the references to color in this figure, the reader is referred to the web version of this article.)

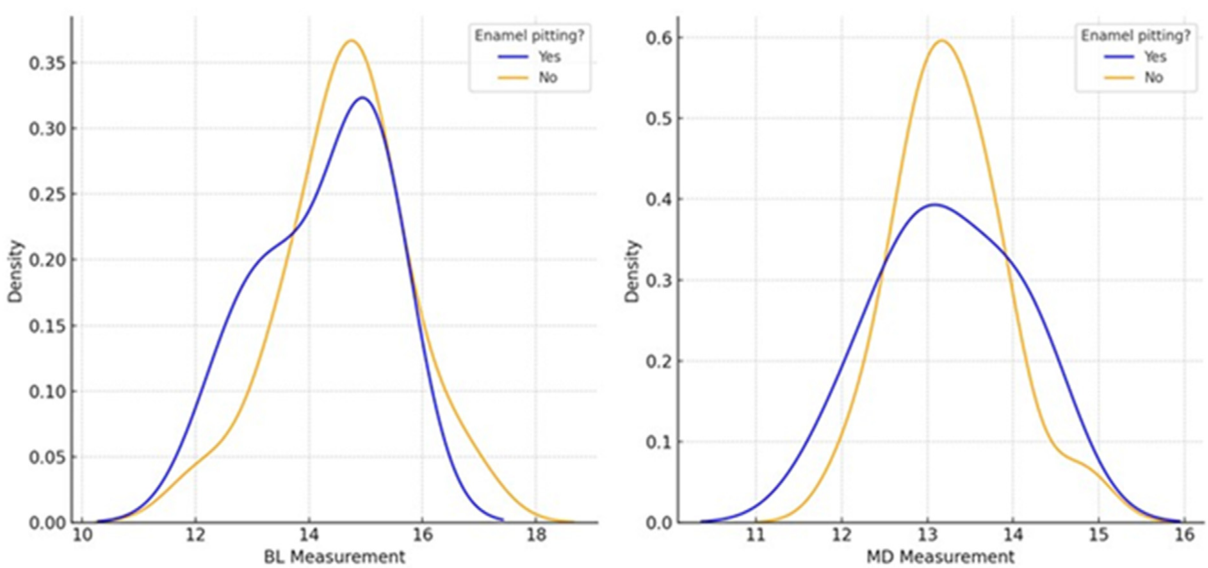

Figure 7. Kernel density estimation (KDE), plotting tooth measurements with UCS pitting, illustrating the relationships between mesial-distal (MD) and buccal-lingual (BL) measurements of teeth (mm), differentiated by the presence or absence of UCS pitting. All samples are upper first molars belonging to *Paranthropus robustus*, from Swartkrans, Drimolen Main Quarry, and Kromdraai (the same specimens as Fig. 6). The KDE plots show the distribution of MD and BL measurements for each enamel pitting category. UCS = uniform, circular, and shallow. (For interpretation of the references to color in this figure, the reader is referred to the web version of this article.)

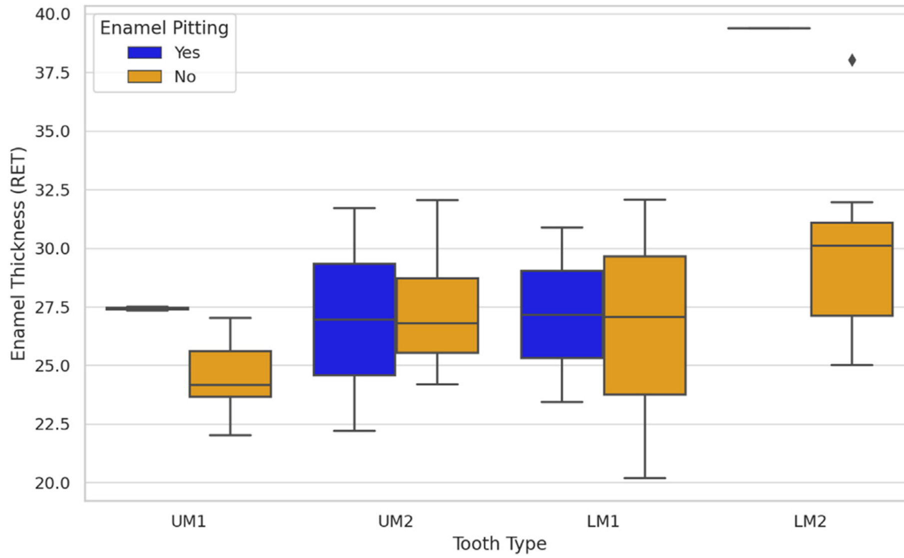

Figure 8. Box and whisker plot of relative enamel thickness (RET) by tooth type and uniform, circular, and shallow pitting status. UM1 = upper first molar; UM2 = upper second molar; LM1 = lower first molar; LM2 = lower second molar. Upper first molar and LM2 are restricted due to small sample size, and the diamond in LM2 is identified as an outlier. All samples belong to *Paranthropus robustus* from both Swartkrans and Drimolen Main Quarry. (For interpretation of the references to color in this figure, the reader is referred to the web version of this article.)

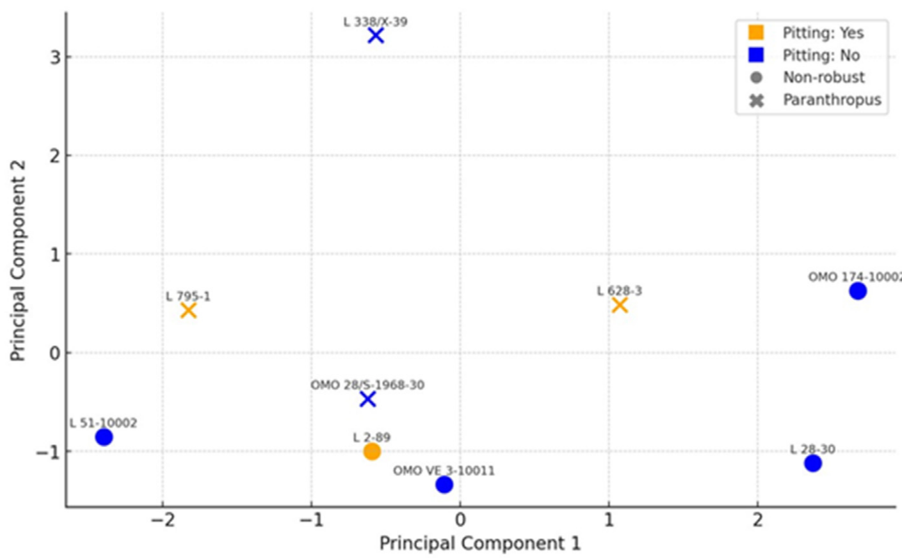

Figure 9. Principal component analysis of lower third molars based on cusp area ratios. All specimens are from Omo and split into *Paranthropus* and non-*Paranthropus* categories (see Table 1). Principal component 1 (PC1) explains 38.18% and principal component 2 (PC2) explains 25.65% of the variance (eigenvalues: PC1 = 3.01; PC2 = 2.02; factor loadings: PC1 [−0.51, 0.47, 0.13, 0.26, 0.52, −0.39, −0.06], PC2 = [−0.20, −0.08, −0.15, −0.56, 0.02, −0.33, 0.71]). (For interpretation of the references to color in this figure, the reader is referred to the web version of this article.)

Table 3
Total occlusal area for lower third molars in the Omo sample.

Specimen number	Group	UCS pitting	Total occlusal area
L 795-1	*Paranthropus*	Yes	259.26
L 628-3	*Paranthropus*	Yes	278.44
OMO 28/S-1968-30	*Paranthropus*	No	228.73
L 338/X-39	*Paranthropus*	No	253.71
L 28-30	Nonrobust	No	176.65
OMO 174-10002	Nonrobust	No	135.07
OMO VE 3-10011	Nonrobust	No	158.98
L 51-10002	Nonrobust	No	170.66
L 2-89	Nonrobust	Yes	145.93

UCS = uniform, circular, and shallow.

4. Discussion

The large sample of isolated teeth from the hominin Omo sequence provides an ideal sample for studying UCS pitting through time and across taxa. This assemblage allows a detailed examination of when pitting occurred and how it correlates with other tooth characteristics. However, the isolated nature of these teeth also means that individual specimens are prone to taxonomic uncertainty, given that the analysis must be based on the anatomy of just that one tooth (a less-than-ideal approach to taxonomic identification; Hlusko et al., 2024). Debates over the taxonomy of individual Omo teeth will continue, with outcomes varying

Table 4
Enamel pitting diameter at the surface (mm).

Specimen	Average	Min	Max
OMO 18-1970-1799	0.16	0.13	0.20
L 26-1G	0.17	0.11	0.21
L 795-1	0.20	0.15	0.28
L 1/nn-10010a	0.16	0.14	0.20
L 2-89	0.18	0.14	0.25
L 64-2	0.14	0.11	0.17
OMO 222-1973-2744 (dm1)	0.17	0.14	0.21
OMO 222-1973-2744 (dm2)	0.16	0.11	0.21
L 704-2	0.18	0.13	0.22
DNH 30	0.22	0.14	0.32
DNH 36	0.17	0.13	0.20
SK 61 (RM1)	0.23	0.12	0.36
SK 89 (LM1)	0.16	0.12	0.26
SK 61 (RdM2)	0.17	0.11	0.28
SK 61 (LdM2)	0.18	0.12	0.26
SK 63 (RdM2)	0.23	0.11	0.42
SK 64 (RdM2)	0.16	0.12	0.21

Data are based on 10 measurements for each sample. The Swartkrans data are from Towle and Irish (2019), using slightly more readings per specimen (15–20 instead of 10).

according to the analytical methods and comparative samples used. For the geologically younger Omo horizons, this uncertainty is reduced by the clear anatomical differences that have evolved between the two main taxonomic groups represented at that time: *Paranthropus* vs. more gracile forms. In contrast, the taxonomic identification of teeth from the older Omo sediments is more difficult. This is to be expected as the closer you get to a last common ancestor, the more difficult it is, by definition, to differentiate incipient species lineages (baboons provide an excellent demonstration of this phenomenon in action, Jolly, 1993). The geologically older Omo sediments yield hominin teeth that are taxonomic puzzles. For example, two teeth that Hlusko et al. (2024) assign to *Paranthropus* from Member B (L 795-1 and OMO 28/s-1968-30) have previously been classified either as indeterminate hominins (Howell and Coppens, 1974; Suwa et al., 1996) or as having affinities with *Australopithecus* (Wood and Leakey, 2011). Given that ancestors are difficult to predict by their descendant species (White et al., 2015), these taxonomic inferences will only be resolved as more fieldwork is conducted and, hopefully, more complete specimens are recovered. Therefore, our taxonomic interpretations for the older fossils must be considered tentative rather than conclusive. With that said, we turn to the detailed discussion of our results.

We have shown here that UCS pitting, characterized by numerous relatively uniform shallow and circular pits on the enamel surface, is common in some hominin species, in both eastern and southern Africa. This pitting has long been recognized in southern African *P. robustus* (Robinson, 1956; White, 1978; Towle and Irish, 2019) but, as we demonstrate here, is also common on postcanine teeth of *Paranthropus* in eastern Africa. We show that UCS pitting is not only restricted to *Paranthropus* but also observed on the postcanine teeth of Late Pliocene *Australopithecus* specimens from the Omo, Ethiopia. Our two hypotheses, that this phenomenon is restricted to *Paranthropus* and associated with specific morphological features such as thicker enamel and larger teeth, are therefore not supported. However, UCS pitting does appear to be restricted to specific taxonomic groups, although not exclusively to *Paranthropus*. Despite UCS pitting being observed across a wide geographic and temporal range, the morphology at Swartkrans, DMQ, and Omo is remarkably similar. This includes postcanine teeth with similar-sized pits and positions in the crown across all individuals affected and a lack of correlation with other aspects of morphology and crown size.

4.1. The pervasiveness of pitting enamel hypoplasia and the uniqueness of uniform, circular, and shallow pitting

Uniform, circular, and shallow pitting and pitting defects more generally are rare in hominins and other nonhuman primates, especially compared to LEH (Colyer, 1936; Hillson and Bond, 1997; Guatelli-Steinberg, 2015; Towle and Irish, 2020). Indeed, defects termed PEH in the literature for nonhuman primates mostly do not fit the definition of UCS pitting. Instead, they are irregular in shape and size or form within LEH bands (Fig. 10). In fact, it is difficult to find examples of UCS pitting in the literature in nonhominin primates. For example, out of several hundred chimpanzees and gorillas studied at the Powell-Cotton Museum, only 1.73% had PEH (Towle and Irish, 2020), and none would be considered UCS pitting (Fig. 10V,W). In a cursory survey of the oral scans for almost 1000 captive baboons from the Southwest National Primate Research Center, only a few were found to have pitting defects (personal observation of I.T. and A.T.), and these pitting defects are associated with other tooth morphology changes (Fig. 10S–U). Similarly, pitting defects in archaeological samples either do not resemble UCS pitting or are associated with severe defects (i.e., plane-form defects) or altered crown morphologies (e.g., Ogden et al., 2007; Towle et al., 2018, Fig. 10O–R). There is no indication that UCS pitting is present in any human sample/population at rates higher than what would be expected with hypoplastic AI (i.e., under 1% of individuals). This rarity is supported by the presence of only one potential case out of >5000 post-Pleistocene African dentitions studied by J.D.I. (personal observation; Fig. 10R).

Although PEH has been identified on teeth of various hominin specimens (e.g., Tobias, 1967; Ogilvie et al., 1989; Xing et al., 2016; Zanolli et al., 2017), at present there is no evidence to support widespread UCS pitting other than what is observed in *Paranthropus* and now in Late Pliocene *Australopithecus*. Pitting on postcanine teeth of *P. robustus* has been observed and described previously (Robinson, 1956; White, 1978; Moggi-Cecchi et al., 2010), and a recent review of South African hominin material found this species to be solely affected by this type of defect (Towle and Irish, 2019). Also, UCS pitting in DMQ, Swartkrans, and Omo teeth with defects consistent with this specific type is visible in published examples of *Paranthropus* and Late Pliocene *Australopithecus* from other sites. This includes *P. boisei* (Tobias, 1967; de Ruiter et al., 2009; Moggi-Cecchi et al., 2010) and material from Lomekwi, Kenya, dated between 3.5 and 3.2 Ma, but currently without firm attribution to a specific species (Skinner et al., 2020). At least two Lomekwi specimens, thought to be antimeres, show pitting consistent with UCS pitting (KNM-WT 38362A and KNM-WT 38362B), based on images in Skinner et al. (2020).

There is no convincing evidence for UCS pitting in *Australopithecus africanus* sensu lato. A small number of *Au. africanus* teeth were recorded for pitting and/or localized enamel defects (Towle and Irish, 2019, 2020), but none (with two possible exceptions, discussed later) fit the features observed in the Omo, Swartkrans, and DMQ teeth. Instead, the few teeth with potential pitting, i.e., PEH within LEH bands (e.g., Stw 132), comprise a small collection of irregular sized and/or shaped defects (e.g., Stw 14, Stw 120, Stw 295, and Stw 404), or the enamel has the 'wavy' appearance (detailed below) that resembles irregular shallow pitting in very localized crown positions (e.g., Stw 332 and Stw 487). Stw 404 is one of the smallest specimens from Sterkfontein Member 4 and was defined as *Au. africanus* by Clarke and Kuman (2019); however, they define Stw 14 as a separate species (*Australopithecus prometheus*) likely ancestral to *Paranthropus*. In all of these examples, it is also difficult to rule out postmortem affects due to their irregularity and minimal expression, and most do not fit commonly used enamel hypoplasia definitions. One possible exception is Stw 140, which shows relatively uniform pitting covering much of the crown. However, even in this case (see Fig. 2 of Towle and Irish, 2020), the pitting appears to form in vertical lines, and within these lines, the PEH are located in regions with general enamel reduction. Additionally, the lower second permanent molars of MLD 2 also display pitting consistent with UCS pitting, but it is fully restricted to the occlusal surface. This specimen is also defined as *A. prometheus* by Clarke and Kuman (2019). Therefore, out of almost 500 *Au. africanus* teeth (Towle and Irish, 2020), no convincing evidence for UCS pitting was found.

The holotype specimen of *Australopithecus bahrelghazali* (KT12/H1) has been described as having PEH (Brunet et al., 2002). No images are provided in this publication (only drawings), but the overall impression from the description, illustrations, and published images available online is that these defects are not consistent with UCS pitting; they seem to mostly form in distinct horizontal bands or are irregular in shape. Therefore, pitting form LEH and/or localized defects may better explain these defects.

Figure 10. Examples of enamel hypoplasia and other dental defects, as well as purely morphological features that somewhat resemble but are not UCS pitting, in hominin and nonhuman primate samples. A) *Pithecia* sp. specimen 4650 (Primate Research Institute, Kyoto University, Japan). Buccal view. Morphological features that can superficially resemble pitting enamel hypoplasia. B) *Pithecia* sp. specimen 4650 (Primate Research Institute, Kyoto University, Japan). Occlusal view. Morphological features that can superficially resemble pitting enamel hypoplasia. C) *Homo antecessor* individual H3, specimen ATD6-69. Enamel hypoplasia (from left to right): right fourth premolar, right canine, and left third premolar. Photo: Elena Lacasa Marquina (Martín-Francés, 2015). Described as pitting enamel hypoplasia in Martín-Francés (2015). D) Peche Neanderthal juvenile, described as having pitting enamel hypoplasia (Ogilvie et al., 1989). However, it does not resemble UCS pitting. Photo: Debbie Guatelli-Steinberg (with permission from Muséum national d'Histoire naturelle, Paris, France). E) Irregular wavy or pitting enamel in an *Australopithecus africanus* right lower lateral incisor (STW 332). F) A couple of individual large pits, which seem antemortem in nature (localized enamel hypoplasia). SK 69 (*Paranthropus robustus*), upper left central incisor. G) 'Wavy' enamel appearance on the buccal surface of a right upper permanent canine (UW 101–501, *Homo naledi*; Towle, 2017). H) Wavy abnormal enamel on the buccal surface of *H. naledi* specimen UW 377/1014 (second molar; Towle, 2017). I) Drimolen Main Quarry (southern Africa), labial of an upper right canine (DNH 108). Multiple LEH bands visible. J) Drimolen Main Quarry (southern Africa), anterior teeth: buccal surface of the lower right canine (DNH 8). Unusual wavy defects that seem antemortem and in places could be described as pitting enamel hypoplasia and/or localized hypoplasia. K) Drimolen Main Quarry (southern Africa), right upper canine labial mesial (DNH 82) displaying LEH. L) Hortus III (Neanderthal; Lumley, 1972; Lumley, 1973). Pitting that resembles UCS pitting but is further down the crown that is affected, which is not seen in *Paranthropus*/Omo (i.e., if further down the crown is affected then so are areas closer to, and on, the occlusal surface). Image by Debbie Guatelli-Steinberg with permission for use from Henry de Lumley. M) Vertical bands of pitting. Left upper third molar (STW 140, *Au. africanus*). N) A few scattered pits of varying size that do not appear to be postmortem in nature. Right lower third molar (STW 2950, *Au. africanus*) but does not resemble UCS pitting. O) Human mandible (Hamann-Todd Osteological Collection; image taken by Debbie Guatelli-Steinberg). Note the USC pitting on the first molar but is associated with severe defects further down the crown and in other teeth, which is not seen in *Paranthropus*/Omo UCS pitting. P) Human upper left second premolar (Roman site in Gloucester, UK; Towle et al., 2018). The lingual surface shows USC pitting but is associated with plane-form defects elsewhere in the dentition. Q) Human upper right central incisor (Neolithic; Barcelona, Spain). Irregular enamel defects. Image by Raquel Hernando. R) Adult female human (Matjes River, P1271; image by Joel D. Irish). Affiliated with Khoesan populations (Irish et al., 2014). Curated at the National Museum in Bloemfontein, Florisbad Research Station. The distal crown surface of the upper first molars has pits that look similar to UCS pitting, but the second and third molars have more severe occlusal alterations, including numerous additional cusplets on the third molars. S) Hamadryas baboon (*Papio hamadryas*), curated at Loyola University, Chicago (W 399). Left maxillary teeth. Note the pitting on the third molar that looks superficially like USC pitting, but elsewhere it looks more like generalized defects. All teeth appear affected except the first molar, likely because it was forming in utero (e.g., see Towle et al., 2023). T) Hamadryas baboon (*P. hamadryas*), curated at Loyola University, Chicago (W 539). Upper left maxillary posterior permanent teeth, buccal view. Pitting is observable on both the second and third molars. The first molar seems unaffected. U) Hamadryas baboon (*P. hamadryas*), curated at Loyola University, Chicago (W 539). Upper left maxillary posterior permanent teeth, occlusal view (same teeth as in (T)). Note irregular pitting in the second and third molars is associated with substantial changes to the morphology of the teeth. The first molar seems unaffected in terms of enamel defects and cusp morphology. V) Chimpanzee (*Pan troglodytes*) showing what could be described as either localized or pitting enamel hypoplasia (curated at the Powell-Cotton Museum: specimen C 195; left upper first deciduous molar). W) Female chimpanzee (*P. troglodytes*; curated at the Powell-Cotton Museum: specimen M 299) showing enamel defects, described as pitting/plane-form defects related to amelogenesis imperfecta in Towle et al. (2018). X) A *Pithecia* canine (curated at the Primate Research Institute, Kyoto University, Japan: PRI 688 *Pithecia* sp.). Buccal view, with an irregular pitted surface that does not fit any commonly used enamel hypoplasia definition. LEH = linear enamel hypoplasia; UCS = uniform, circular, and shallow. (For interpretation of the references to color in this figure, the reader is referred to the web version of this article.)

There are individual teeth of *Homo* from Eurasia and the Middle East recorded as displaying PEH or showing apparent pitting in published images, but typically they do not fit the description of UCS pitting. Often, irregular pitting across parts of the crown or single large pits are present; anterior teeth are also often affected (incisors and canines), including in association with LEH (e.g., Puech and Albertini, 1981; Trinkaus, 1987; Ogilvie et al., 1989; Bailey and Hublin, 2006; Glantz et al., 2008; Guatelli-Steinberg et al., 2013; Martín-Francés, 2015; Blinkhorn et al., 2021; Martín-Francés et al., 2022). Molnar and Molnar (1985) describe PEH in the Krapina Neanderthals, although it is predominantly in the anterior teeth, and it seems many of the examples may be associated with LEH (e.g., their Fig. 4). Possible defects of a similar type were described by Ogilvie et al. (1989), in which half of the defects in the posterior teeth of Neanderthals were classified as pitting. However, many are just a single large irregular pit (many of which would likely now be classified as localized enamel hypoplasia) and often associated with LEH. Even the specimens recorded as having multiple pits do not seem consistent with UCS pitting described in the present study (e.g., see Fig. 10 of Pech-de-l'Aze 1; potential exceptions discussed below).

Some *Homo* teeth with substantial cusplets, crenulations, or folding of the occlusal surface can also display features that superficially resemble enamel pitting. Pitlike features can be found in relation to cusp tips and occlusal fissures (pits forming where multiple developmental lines converge; Bekes et al., 2018), all of which are typically restricted to the occlusal surface (e.g., Glantz et al., 2008; Smith et al., 2009; Martin et al., 2017; Henrion et al., 2023; Davies et al., 2024). In some cases, these specimens show defects superficially like UCS pitting, with the caveat that these are typically limited to a few pits and typically not clustered together like the *Paranthropus*/Late Pliocene *Australopithecus* examples. This includes Neanderthal, where in some posterior teeth, the occlusal surface, and occasionally other surfaces, is affected (e.g., Krapina D170 third molar and El sidrom SD 621 third molar, Martin et al., 2017); the same applies to an early *Homo* specimen (OH 16 third molars, Davies et al., 2024).

However, there are examples of *Homo* in which UCS pitting does seem to be present. The most similar published example is in Xing et al. (2016), where enamel pitting similar to UCS is found on an upper premolar and second molar of a Late Pleistocene juvenile from Xujiayao, China. Other enamel defects are present in this individual, including localized enamel hypoplasia and LEH in the anterior dentition. The species designation of this fossil is debated, but it has been suggested to represent an unknown hominin lineage distinct from contemporaneous *Homo sapiens* and *Homo neanderthalensis* (Wu, 2024); it was recently suggested to represent a distinct *Homo* species, *Homo juluensis* (Bae and Wu, 2024). Regardless, it is currently the only convincing published description of UCS pitting outside the present study we could find in the literature. In addition to this fairly certain identification of UCS pitting, there are some specimens within *Homo* that may represent UCS pitting. A Neanderthal specimen that appears to display defects similar to UCS pitting is Hortus III, although there is some irregularity in the pitting, and it is further down the crown (Fig. 10L). Pitting that looks similar to UCS pitting is also found in *Homo floresiensis* (both LB1 and LB6/1) based on the high-resolution images in Kaifu et al. (2015a,b). Unfortunately, dental wear, with the cusps mostly removed, makes comparisons difficult using these images. Yet the fact that both individuals potentially display UCS pitting is worth exploring. The specimen identified as *Homo* aff. *erectus*, GAR IVE from the c. 1.7-Ma-old Garba IV site at Melka Kunture (Upper Awash Basin, Ethiopia) has been described as having AI (Zilberman et al., 2004). Based on high-resolution images in Zanolli et al. (2017), it is possible these defects could be consistent with UCS pitting. However, a detailed study of the original material is required as the defects may be more irregular than those described in the present study.

The paucity of different types of enamel pitting in *Homo* and *Au. africanus* is consistent with normal 'stress'-related PEH, as well as the inclusion of localized defects in some descriptions/studies. Indeed, the mix of LEH, pitting, plane form, and localized defects described in hominins (excluding *Paranthropus*), is in line with ratios of defects expected based on human and extant primate studies that compared hypoplasia types across populations (e.g., Lukacs, 2001a,b; Towle and Irish, 2020; Samuel et al., 2023). In certain cases, an AI etiology seems likely, which again is in line with current estimates for recent human populations. That is, the frequency is less than one in 100 individuals with this genetic condition. However, a more thorough study, like that of the South African and Omo specimens, is required for other eastern African sites and Eurasian hominins to confirm UCS pitting prevalence. A few likely examples, as noted, suggest UCS pitting is present in other fossil hominins as it is in archaeological and clinical human samples (Fig. 10). The latter are rare, associated only with certain diseases and genetic disorders (mentioned later in the text).

Unlike Towle and Irish (2019), we did not include anterior teeth (incisors and canines) in our study. These anterior teeth from DMQ show substantial LEH, but other defect types including some that might be pitting or localized hypoplasia are present (Fig. 10I–K). Robinson (1956) and White (1978) also suggested the anterior teeth of 'robust' specimens showed more common enamel defects than 'nonrobust' ones, although more recent research found similar rates or the reverse pattern (Guatelli-Steinberg, 2003; Towle and Irish, 2019). Upon macroscopic examination, these potential anterior tooth defects show little similarity to the UCS pitting described here. Often, like other fossil hominin samples, 'wavy' irregular enamel is evident that does not adequately fit within common hypoplasia categories (plane form, linear, pit, and localized). A study focusing on enamel defects (and surface morphology) on complete dentitions is required to understand these features and their potential association with UCS pitting. However, based on common enamel defect categories, there does not seem to be evidence for an increase on the anterior teeth in species commonly showing UCS pitting; this impression is based on LEH comparisons between *P. robustus* and *Au. africanus* (e.g., Guatelli-Steinberg, 2004; Towle and Irish, 2019).

4.2. Uniform, circular, and shallow pitting etiology

The identification of UCS pitting as a specific type of enamel morphology raises questions about its etiology. *Paranthropus* and *Australopithecus* UCS pitting does not resemble hypoplastic defects found in typical modern clinical cases of PEH, including those often associated with premature birth, low birth weight, vitamin D deficiency, tuberous sclerosis, congenital syphilis, pseudohypoparathyroidism, and epidermolysis bullosa (Croft et al., 1965; Purvis et al., 1973; Stimmler et al., 1973; Seow et al., 1984; Wright et al., 1993; Gaul et al., 2015; Radu and Soficaru, 2016). Most of these conditions are associated with pitting that is irregular in both shape and distribution. These medical conditions also affect all teeth, not just the postcanine dentition, and are typically associated with other types of severe dental defects. These defects often penetrate much deeper into the enamel than *Paranthropus* UCS pitting by as much as one-third of the full enamel thickness (Arwill et al., 1965; Hoff et al., 1975; Paulson et al., 1984).

Dental fluorosis Enamel pitting defects have also been associated with deficiencies or surpluses of certain compounds, including dental fluorosis, mercury poisoning, and calcium deficiency (Fejerskov et al., 1990; Schultz et al., 1998; Ogden et al., 2007; Ioannou et al., 2015; Radu and Soficaru, 2016). With that said, *Paranthropus* and Late Pliocene *Australopithecus* UCS pitting is superficially similar to some of these examples, so a specific environmental or dietary component, or absence thereof, cannot be completely ruled out.

Dental fluorosis, in particular, is worth consideration, even though it typically manifests as irregular pitting—in some cases appearing similar to UCS pitting. Despite extensive research, the mechanisms behind dental fluorosis remain incompletely understood (Martinez-Mier et al., 2016; Marchenko et al., 2024). It is clear, however, that elevated fluoride intake is a factor, with clinical presentations varying by severity. Across the mammal taxa studied, fluoride-induced changes commonly include discoloration and structural or mineralization alterations (e.g., Kierdorf et al., 1996; Aoba and Fejerskov, 2002; Kierdorf et al., 2004; Everett et al., 2011; Charone et al., 2019). In severe cases, pitting becomes a key marker of dental fluorosis but is seemingly always accompanied by other dental alterations, such as coloration changes, obvious histological and surface mineralization changes, or associated atypical wear patterns (Aoba and Fejerskov, 2002; Kierdorf et al., 2004; Bronckers et al., 2009). Histological studies have shown how these structural changes often produce uniform enamel and affect the appearance of specific histological features (e.g., Hunter-Schreger bands; striae of Retzius) or else show modified enamel prism morphology/structure (Marchenko et al., 2024).

The UCS pitting in the present study is not associated with any of these additional alterations. We see no evidence of atypical wear or obvious mineralization or coloration changes or changes to enamel thickness or overall morphology of the crown. Although taphonomic processes might obscure some of these factors, especially coloration, the major structural or wear differences expected based on clinical expression of severe fluorosis would be evident on the fossils. Additionally, based on synchrotron imaging in Smith et al. (2015), which included specimens identified in the present study with UCS pitting, there are no clear enamel structural differences between teeth with and without pitting (based on individual two-dimensional slices for particular crown positions; online supplemental files, Smith et al., 2015). Similarly, in an article on the *P. robustus* specimen SK 63 (Dean et al., 1993) with UCS pitting on the posterior teeth, the histology of the canine (without UCS pitting but has overlapping developmental times with the teeth that do) shows no alterations in enamel structure consistent with severe fluorosis. These examples provide only circumstantial evidence but do suggest that dental fluorosis is unlikely to be the etiology of UCS pitting.

Indeed, the connection between fluorosis and an individual with the UCS pitting is not new: A pit on the Xujiayao juvenile's central incisor (the only *Homo* individual with a fairly certain identification of UCS pitting) was originally suggested to be fluorotic (Chia et al., 1979). However, Xing et al. (2016) evaluated this claim extensively and determined that the teeth did not exhibit features consistent with fluorosis. And, in a subsequent synchrotron analysis of the same individual (Xing et al., 2019), the internal enamel structure did not reveal any mineralization defects or deviations from normal.

It is worth noting that there is a genetic component to the susceptibility of dental fluorosis in humans and other mammals, not just at the individual level but also between populations (Huang et al., 2008; Everett et al., 2008, 2011; Ba et al., 2011; Jiang et al., 2015; Küchler et al., 2018; Charone et al., 2019). Therefore, it is possible that the enamel in these hominins is more susceptible to a particular environmental stimulus (e.g., exposure to high levels of fluoride in drinking water). This could be in relation to elevated levels compared to other populations (i.e., relating to geology of the local environment) or due to a physiological process in which fluoride (even at low levels) puts individuals at risk of accumulating toxic levels.

<u>Environmentally based physiological stressor</u> Tobias (1967) considered all enamel hypoplasia in *P. boisei* individuals to share an etiology, relating at least partly to chronic illness during dental development. At present, we consider episodic physiological stress to be less likely and suggest UCS pitting is most consistent with a primarily genetic etiology due to six observations: 1) UCS pitting is not associated with similar pitting or elevated LEH frequencies on incisors and canines (as observed in direct comparisons of the Swartkrans material; Towle and Irish, 2019); 2) the remarkable uniformity of pitting across affected teeth (both deciduous and permanent); 3) resemblance of defects to those in human cases of a specific subtype of AI that results from a genetic variant; 4) the lack of evidence for reduced tooth size or enamel thickness in affected teeth, which might be expected with severe malnutrition or illness during dental development; 5) the pattern of UCS pitting on the crowns does not show the horizontal anomalies associated with a specific time of disruption to enamel development (LEH or bands of PEH; Schulze, 1970; Paulson et al., 1984); and 6) UCS pitting is often expressed in the cusp region of different posterior teeth that do not form concurrently during dental development, which is inconsistent with an environmentally induced episode of disruption.

<u>Amelogenesis or enamel structural cause</u> Another possible explanation for UCS pitting could result from the observation that apoptosis of ameloblasts nearing enamel completion can be more susceptible to stress (Lacruz et al., 2017). The deep LEH (in DMQ) and potential irregular defects on the aforementioned anterior teeth (see Fig. 10) could be evidence of a specific environmental trigger being common in these individuals. Further research comparing these features on anterior and posterior teeth is required to access any associations. For example, Witzel et al. (2006) identify a single accentuated line stress event close to the outer enamel surface underlying multiple pits in pig teeth. Studies that explored environmental, seasonal, and developmental changes through the course of an individual's lifespan may help address this possibility (e.g., Paine et al., 2019; Dean et al., 2020; Green et al., 2022).

Tobias (1967) suggested that UCS pitting could be associated with the formation of crenulations. For example, *Pithecia* and *Pongo* molars regularly show crenulations, and similar undulating enamel can be observed in fossil apes, such as *Rangwapithecus gordoni*. However, this association may not apply to *Paranthropus* as this taxon is often characterized by a simplification of occlusal morphology rather than an increase in the complexity of the occlusal surface associated with crenulation. Additionally, crenulation and crenation may be related to the thickening of enamel in relation to the occlusal geometry and may have a precursor at the EDJ (Guy et al., 2015). In some of these extant and extinct primates with crenulation, the crown seems to be covered with pitting and similar 'defects' (both occlusal and nonocclusal surfaces), but these morphologies are actually related directly to normal tooth morphology (Fig. 10A,B). Interestingly, in these primate examples of crenulation, expression seems variable, with, for example, some *Pithecia* showing smooth buccal and lingual surfaces in posterior teeth, while others having marked 'pitting' and vertical depressions.

Another aspect of crown and especially cuspal and occlusal development that needs to be discussed is cusp tip pit(s) (CTPs). These pits on the apex of cusps are restricted to the enamel (Ruben et al., 2019; de Sousa and Hara, 2023). Paulson et al. (1984) described how CTPs often relate to one large pit directly in the center of the cusp tip, though a collection of small uniform pits can occur there. It is therefore worth noting that some DMQ, Swartkrans, and Omo teeth with UCS pitting also show CTPs (personal observation, I.T. and M.C.O.). Pits were also found in fusion lines of human posterior teeth, again with an enamel formation etiology (Paulson et al., 1984). Although UCS pitting often covers large areas of the crowns in Omo and South African samples, it is often most visible in occlusal fissures or cuspal areas with undulating or convex surfaces and therefore may be related to CTPs.

Both the morphology of the posterior teeth and speed of enamel formation may be part of the UCS pitting and CTP features. For example, at the cusp tips, the ameloblasts and resulting prisms are larger than those on the surrounding surfaces (Paulson et al., 1984). Similar variation in prism width, from the EDJ to the resulting size at the outer enamel surface, was found to vary by crown position (Towle and Loch, 2024). Paulson et al. (1984) proposed that the central core area of the cusp tip may progressively lag behind in matrix deposition because of fewer ameloblasts per unit area than in the immediately adjacent cusp slope matrix. Following this logic, as with CTP, UCS pitting in *P. robustus* and Omo samples could relate to the rounded convex surface, where ameloblasts did not synthesize sufficient matrix. Therefore, these pits could result from widely separated ameloblasts unable to synthesize sufficient enamel matrix. This would explain why the pits are so shallow and of uniform depth, since they would only affect the finalization of enamel formation. It would also explain why they are so uniformly circular.

Genetics Tobias (1967) supported the notion of a strong genetic underpinning to UCS pitting, including pitting on the posterior teeth. He highlighted the work of Colyer (1936), in which the role of heredity is suggested as a major component. Therefore, our proposal for a unique pitting type pattern in some hominins is not dissimilar from that of Tobias (1967) for *P. boisei*: ‘Thus, it may be suggested that the genotype, the developmental stage of the organism, and the adverse environmental circumstances are jointly responsible for such a pattern of hypoplasia as “*Zinjanthropus*” [*P. boisei*] shows.’ Here we go a step further, suggesting the genetic component is the predominant factor for UCS pitting in these hominins.

Towle and Irish (2019) suggested the rapid evolution of thick enamel in *Paranthropus* could be a cause of UCS pitting, since strong selection on a particular feature can lead to loss of genomic stability in particular genes or create pleiotropy effects on other characteristics (Pavličev and Cheverud, 2015; Fiddes et al., 2018; Hlusko et al., 2018). This interpretation leads to two hypotheses. First is that thick enamel and large posterior tooth size are uniquely associated with this pitting. This is not supported as we see UCS pitting in earlier *Australopithecus* specimens not considered to be robust hominins (Skinner et al., 2015; Lockey et al., 2020). The second hypothesis is that the developmental instability associated with intense selection would be deleterious to some degree as enamel defects often predispose teeth to caries and extreme wear, compromising functionality (Towle et al., 2021). Our study shows that UCS pitting was common for millions of years, with population occurrences likely close to half, particularly for *Paranthropus* (this study; Towle and Irish, 2019). Given this long duration, high frequencies through time, and wide geographic range in this lineage, UCS pitting may not be a pathology per se, even if it does appear to be associated with evidence of illness/disease, inlcuding dental caries. Uniform, circular, and shallow pitting may instead be a trait or characteristic, in a similar manner to nonmetric dental traits and crenulations.

Research on human health suggests that UCS pitting could be a type of AI, though one that occurred at a much higher frequency than in humans. Today, AI affects approximately one in every 700 to 14,000 people (Sundell and Koch, 1985; Crawford et al., 2007). Defects usually include scattered pits and plane-form hypoplasia; abnormal coloration, thickness, and density of the enamel are also common (Wright, 1985; Aldred et al., 2003; Smith et al., 2017). A specific type of AI, hypoplastic amelogenesis imperfecta (Wright et al., 1993; Mehta et al., 2013), most closely emulates UCS pitting in fossil hominins, in that it commonly does not show discoloration or abnormalities in enamel thickness or density (Witkop and Sauk, 1976; Witkop, 1988; Seow, 1993). A recent study highlights a particular genetic mutation that causes presence of defect on posterior but not anterior primary teeth (Kim et al., 2016), a pattern that matches what we observe on the fossils.

A similar explanation could relate to an AI type proposed to be associated with cuspal areas in humans, related to areas receiving the greatest increase in enamel volume via ameloblasts from the EDJ to outer enamel (Poulter et al., 2014). Therefore, a genetic underpinning (e.g., from AI or pleiotropy) could cause this pitting but only affect crown areas experiencing substantial changes in enamel volume moving outward in the crown, especially those with undulating or convex surfaces. Enamel decussation may also be an important factor, given its effect on the enamel prism process (length and time). Both enamel formation hypotheses would explain why the cuspal areas in Omo and *Paranthropus* samples are often affected, as well as other areas having undulating enamel between cusps on the buccal and lingual surfaces. Taken together, we suggest UCS pitting on these hominin teeth relates to specific enamel formation processes. However, further research is required to test the hypotheses proposed here, including through histological, microscopy, and nano-CT techniques.

4.3. *Possible implications*

Irrespective of its potential connection to pleiotropy or specific enamel formation processes, if caused primarily by a genetic effect or susceptibility, UCS pitting appears confined to, or at least much more common in *Paranthropus* and eastern African Late Pliocene *Australopithecus*. It seems unlikely that such a specific feature would appear twice in the hominin record. The simplest explanations are that other hominins (including *Homo* and *Au. africanus*) 1) lost this feature, 2) do not express it due to alterations in physiology and/or tooth development, or 3) diverged from the lineage before its appearance. These results therefore lend some support to the monophyletic grouping for *Paranthropus*, with the most parsimonious explanation being that this lineage evolved from an eastern African Late Pliocene *Australopithecus*, like *Australopithecus afarensis*.

Even if UCS pitting is heritable, multiple evolutionary processes and phylogenetic factors must be considered before it can be confidently applied to hominin taxonomy. Thus, further research into the genetic underpinnings of the UCS phenotype is needed. If subsequent studies continue to support our genetic/enamel formation hypothesis, UCS pitting may ultimately prove to be a useful trait marker for use in hominin phylogenetic reconstructions.

5. Conclusions

This study presents an analysis of enamel pitting in early hominins, focusing on a distinct form initially identified in *P. robustus*, and extending the investigation to other fossil hominins in Africa. Our findings show that this specific type of pitting, which we name UCS pitting—characterized by circular uniform shallow pitting—is common in both eastern and southern African *Paranthropus* taxa and is observable in eastern African Late Pliocene *Australopithecus* taxa. Uniform, circular, and shallow pitting is absent or rare in other *Australopithecus* and fossil *Homo* taxa. Our results do not support a correlation between the presence of enamel pitting and variation in tooth size, enamel thickness, or cusp proportions. The consistent appearance of this pitting type in

Paranthropus and early *Australopithecus* across different paleontological sites may suggest a shared genetic basis related to enamel formation, potentially in association with specific environmental or dietary factors. This, in turn, may offer a novel phenotype for use in hominin taxonomy.

Declaration of competing interest

The authors have no competing interests to declare.

Acknowledgments

This research was supported by funding from the European Research Council (ERC) within the European Union's Horizon Europe (ERC-2021-ADG, Tied2Teeth, project number: 101054659), a grant from the Spanish Ministerio de Ciencia e Innovación (Project PID2021-122355NB-C33 financed by MCIN/AEI/10.13039/501100011033/FEDER, UE), and support from the France-Berkeley Fund (2018 to J.R.B. and L.J.H.). The participation of M.C.O. was supported by the National Science Foundation Graduate Research Fellowship Program (grant number: DGE-1343012) and the European Union's Horizon 2020 research and innovation programme under the Marie Skłodowska-Curie grant agreement No 101026776. Any opinions, findings, and conclusions or recommendations expressed in this material are those of the author and do not necessarily reflect the views of the National Science Foundation or the ERC. We also thank the Australian Academy of the Humanities for providing funding that allowed A.B.L. to collect hypoplasia data on the Drimolen Main Quarry specimens. Funding for work at Drimolen Main Quarry was provided by Australian Research Council Discovery Project DP170100056 to A.I.R.H. Access to collections and Omo Group Research Expedition (OGRE) fieldwork permits were granted by the Ethiopian Heritage Authority (EHA). The OGRE is a joint program of PALEVOPRIM, the Centre for Ethiopian Studies, and the EHA, principally funded by the Ministry of Europe and Foreign Affairs, the National Research Agency, the Région Nouvelle-Aquitaine, Centre national de la recherche scientifique Ecology and Environment, PALEVOPRIM, and the Fyssen Foundation. The OGRE is extremely grateful to the EHA, the Southern Nations, Nationalities and Peoples' Region, the South Omo Zone, the Nyangatom and Dassanetch Weredas, and their people for their help and reception.

Author contributions

Ian Towle: Writing – review & editing, Writing – original draft, Validation, Resources, Project administration, Methodology, Investigation, Formal analysis, Data curation, Conceptualization. **Mackie C. O'Hara:** Writing – review & editing, Writing – original draft, Resources, Methodology, Investigation, Formal analysis. **A.B. Leece:** Writing – review & editing, Resources, Methodology, Investigation, Formal analysis. **Andy I.R. Herries:** Writing – review & editing, Resources, Methodology, Investigation, Formal analysis. **Afua Adjei:** Writing – review & editing, Resources, Investigation. **Debbie Guatelli-Steinberg:** Writing – review & editing, Writing – original draft, Resources, Investigation. **Marina Martínez de Pinillos:** Writing – review & editing, Validation, Investigation, Conceptualization. **Mario Modesto-Mata:** Writing – review & editing, Validation, Investigation. **Arthur Thiebaut:** Writing – review & editing, Validation, Investigation. **Raquel Hernando:** Writing – review & editing, Validation, Investigation. **Joel D. Irish:** Writing – review & editing, Writing – original draft, Resources, Methodology, Investigation. **Franck Guy:** Writing – review & editing, Writing – original draft, Resources, Investigation, Funding acquisition. **Jean-Renaud Boisserie:** Writing – review & editing, Writing – original draft, Resources, Project administration, Investigation, Funding acquisition. **Leslea J. Hlusko:** Writing – review & editing, Writing – original draft, Validation, Resources, Project administration, Methodology, Investigation, Funding acquisition, Conceptualization.

Data accessibility statement

The data that support the findings of this study are available in the Results section and SOM of this article. The data are also available through Dryad (Towle et al., 2025).

Supplementary Online Material

Supplementary Online Material to this article can be found online at https://doi.org/10.1016/j.jhevol.2025.103703.

References

Aldred, M.J., Savarirayan, R., Crawford, P.J.M., 2003. Amelogenesis imperfecta: A classification and catalogue for the 21st century. Oral Dis. 9 (1), 19–23.
Aoba, T., Fejerskov, O., 2002. Dental fluorosis: Chemistry and biology. Crit. Rev. Oral Biol. Med. 13 (2), 155–170.
Arambourg, C., Coppens, Y., 1968. Decouverte D'un Australophecien Nouveau Dans Les Gisements De Lomo (Ethiopie). S. Afr. J. Sci. 64 (2), 58.
Arwill, T., Bergenholtz, A., Olsson, O., 1965. Epidermolysis bullosa hereditaria: III. A histologic study of changes in teeth in the polydysplastic dystrophic and lethal forms. Oral Surg. Oral Med. Oral Pathol. 19 (6), 723–744.
Asfaw, B., White, T., Lovejoy, O., Latimer, B., Simpson, S., Suwa, G., 1999. *Australopithecus garhi*: a new species of early hominid from Ethiopia. Science 284 (5414), 629–635.
Bailey, S.E., 2004. A morphometric analysis of maxillary molar crowns of Middle-Late Pleistocene hominins. J. Hum. Evol. 47 (3), 183–198.
Ba, Y., Zhang, H., Wang, G., Wen, S., Yang, Y., Zhu, J., Ren, L., Yang, R., Zhu, C., Li, H., Cheng, X., Cui, L., 2011. Association of dental fluorosis with polymorphisms of estrogen receptor gene in Chinese children. Biol. Trace Elem. Res. 143, 87–96.
Bae, C.J., Wu, X., 2024. Making sense of eastern Asian Late Quaternary hominin variability. Nat. Commun. 15 (1), 9479.
Bailey, S.E., Hublin, J.J., 2006. Dental remains from the Grotte du Renne at Arcy-sur-Cure (Yonne). J. Hum. Evol. 50, 485–508.
Bekes, K., Tangl, S., Dobsak, A., Gruber, R., 2018. The morphology of pits and fissures. In: Pit and Fissure Sealants. Springer International Publishing, Cham, pp. 11–21. https://doi.org/10.1007/978-3-319-71979-5_2.
Blinkhorn, J., Zanolli, C., Compton, T., Groucutt, H.S., Scerri, E.M., Crété, L., Stringer, C., Petraglia, M.D., Blockley, S., 2021. Nubian Levallois technology associated with southernmost Neanderthals. Sci. Rep. 11 (1), 2869.
Bobe, R., Leakey, M.G., 2009. Ecology of Plio-Pleistocene mammals in the Omo-Turkana Basin and the emergence of *Homo*. In: Grine, F.E., Fleagle, J.G., Leakey, R.E. (Eds.), The First Humans: Origins of the Genus Homo. Springer, New York, pp. 173–184.
Boisserie, J.R., Guy, F., Delagnes, A., Hlukso, L.J., Bibi, F., Beyene, Y., Guillemot, C., 2008. New palaeoanthropological research in the Plio-Pleistocene Omo group, lower Omo Valley, SNNPR (southern nations, nationalities and people regions), Ethiopia. C. R. Palevol 7 (7), 429–439.
Bronckers, A.L.J.J., Lyaruu, D.M., DenBesten, P.K., 2009. The impact of fluoride on ameloblasts and the mechanisms of enamel fluorosis. J. Dent. Res. 88 (10), 877–893.
Brophy, J.K., Moggi-Cecchi, J., Matthews, G.J., Bailey, S.E., 2021. Comparative morphometric analyses of the deciduous molars of *Homo naledi* from the Dinaledi Chamber, South Africa. Am. J. Phys. Anthropol. 174 (2), 299–314.
Brunet, M., Fronty, P., Sapanet, M., de Bonis, L., Viriot, L., 2002. Enamel hypoplasia in a Pliocene hominid from Chad. Connect. Tissue Res. 43 (2–3), 94–97.
Charone, S., Küchler, E.C., Leite, A.D.L., Silva Fernandes, M., Taioqui Pelá, V., Martini, T., Brondino, B.M., Magalhães, A.C., Dionisio, T.J., Santos, C.F., Buzalaf, M.A.R., 2019. Analysis of polymorphisms in genes differentially expressed in the enamel of mice with different genetic susceptibilities to dental fluorosis. Caries Res. 53 (2), 228–233.
Chia, L., Wei, Q., Li, C., 1979. Report on the excavation of Hsuchiayao Man site in 1976. Vertebr. Palasiat. 17, 277–293.
Clarke, R.J., Kuman, K., 2019. The skull of StW 573, a 3.67 Ma *Australopithecus prometheus* skeleton from Sterkfontein Caves, South Africa. J. Hum. Evol. 134, 102634.
Collins Cook, D., 1980. Hereditary enamel hypoplasia in a prehistoric Indian child. J. Dent. Res. 59, 1522.
Colyer, F., 1936. Variations and Diseases of the Teeth of Animals. Bale and Danielsson, London.
Condemi, S., 2004. The garba IV E mandible. In: Studies on the Early Paleolithic Site of Melka Kunture, Ethiopia. Origines, Firenze, pp. 687–701.
Crawford, P.J., Aldred, M., Bloch-Zupan, A., 2007. Amelogenesis imperfecta. Orphanet J. Rare Dis. 2 (1), 1–11.

Croft, L.K., Witkop Jr., C.J., Glas, J.E., 1965. Pseudohypoparathyroidism. Oral Surg. Oral Med. Oral Pathol. 20 (6), 758–770.
Cunha, E., Rozzi, F.R., Bermúdez de Castro, J.M., Martinón-Torres, M., Wasterlain, S.N., Sarmiento, S., 2004. Enamel hypoplasias and physiological stress in the Sima de los Huesos Middle Pleistocene hominins. Am. J. Phys. Anthropol. 125 (3), 220–231.
Davies, T.W., Gunz, P., Spoor, F., Alemseged, Z., Gidna, A., Hublin, J.J., Kullmer, O., Plummer, W.P., Zanolli, C., Skinner, M.M., 2024. Dental morphology in *Homo habilis* and its implications for the evolution of early Homo. Nat. Commun. 15 (1), 286.
Dean, M.C., Beynon, A.D., Thackeray, J.F., Macho, G.A., 1993. Histological reconstruction of dental development and age at death of a juvenile *Paranthropus robustus* specimen, SK 63, from Swartkrans, South Africa. Am. J. Phys. Anthropol. 91 (4), 401–419.
Dean, C., Zanolli, C., Le Cabec, A., Tawane, M., Garrevoet, J., Mazurier, A., Macchiarelli, R., 2020. Growth and development of the third permanent molar in *Paranthropus robustus* from Swartkrans, South Africa. Sci. Rep. 10 (1), 19053.
de Ruiter, D.J., Pickering, R., Steininger, C.M., Kramers, J.D., Hancox, P.J., Churchill, S.E., Berger, L.R., Backwell, L., 2009. New Australopithecus robustus fossils and associated U-Pb dates from Cooper's cave (Gauteng, South Africa). J. Hum. Evol. 56 (5), 497–513.
de Sousa, F.B., Hara, A.T., 2023. New theory illustrates the formation of enamel CUP-shaped lesions on occlusal surfaces. Caries Res. 57 (1), 87–94.
Eversole, L.R., 1984. Clinical Outline of Oral Pathology: Diagnosis and Treatment. Lea & Febiger, Philadelphia.
Everett, E.T., Yan, D., Weaver, M., Liu, L., Foroud, T., Martinez-Mier, E., 2008. Detection of dental fluorosis-associated quantitative trait loci on mouse chromosomes 2 and 11. Cells Tissues Organs 189 (1–4), 212–218.
Everett, E.T., Yin, Z., Yan, D., Zou, F., 2011. Fine mapping of dental fluorosis quantitative trait loci in mice. Eur. J. Oral Sci. 119, 8–12.
Fejerskov, O., Manji, F., Baelum, V., 1990. The nature and mechanisms of dental fluorosis in man. J. Dent. Res. 69 (2), 692–700.
Fiddes, I.T., Lodewijk, G.A., Mooring, M., Bosworth, C.M., Ewing, A.D., Mantalas, G.L., Novak, A.M., van den Bout, A., Bishara, A., Rosenkrantz, J.L., Lorig-Roach, R., Field, A.R., Haeussler, M., Russo, L., Bhaduri, A., Nowakowski, T.J., Pollen, A.A., Dougherty, M.L., Nuttle, X., Addor, M.C., Zwolinski, S., Katzman, S., Kriegstein, A., Eichler, E.E., Salama, S.R., Jacobs, F.M.J., Haussler, D., 2018. Human-specific NOTCH2NL genes affect notch signaling and cortical neurogenesis. Cell 173 (6), 1356–1369.
Gaul, J.S., Grossschmidt, K., Gusenbauer, C., Kanz, F., 2015. A probable case of congenital syphilis from pre-Columbian Austria. Anthropol. Anzeiger 72 (4).
Glantz, M., Viola, B., Wrinn, P., Chikisheva, T., Derevianko, A., Krivoshapkin, A., Islamov, U., Suleimanov, R., Ritzman, T., 2008. New hominin remains from Uzbekistan. J. Hum. Evol. 55 (2), 223–237.
Goodman, A.H., Armelagos, G.J., Rose, J.C., 1980. Enamel hypoplasias as indicators of stress in three prehistoric populations from Illinois. Hum. Biol. 52, 515–528.
Goodman, A.H., Armelagos, G.J., Rose, J.C., 1984. The chronological distribution of enamel hypoplasias from prehistoric Dickson Mounds populations. Am. J. Phys. Anthropol. 65 (3), 259–266.
Goodman, A.H., Rose, J.C., 1991. Dental enamel hypoplasias as indicators of nutritional status. In: Kelley, M.A., Larsen, C.S. (Eds.), Advances in Dental Anthropology. Wiley-Liss, New York, pp. 279–293.
Green, D.R., Ávila, J.N., Cote, S., Dirks, W., Lee, D., Poulsen, C.J., Williams, I.S., Smith, T.M., 2022. Fine-scaled climate variation in equatorial Africa revealed by modern and fossil primate teeth. Proc. Natl. Acad. Sci. 119 (35), e2123366119.
Grine, F.E., Leakey, M.G., Gathago, P.N., Brown, F.H., Mongle, C.S., Yang, D., …, Leakey, L.N., 2019. Complete permanent mandibular dentition of early Homo from the upper Burgi Member of the Koobi Fora Formation, Ileret, Kenya. J. Hum. Evol. 131, 152–175.
Guatelli-Steinberg, D., 2015. Dental stress indicators from micro- to macroscopic. In: Irish, J.D., Scott, G.R. (Eds.), A Companion to Dentalanthropology. Wiley-Blackwell, Hoboken, pp. 450–464.
Guatelli-Steinberg, D., Buzhilova, A.P., Trinkaus, E., 2013. Developmental stress and survival among the Mid Upper Paleolithic Sunghir children: Dental enamel enamelplasias of Sunghir 2 and 3. Int. J. Osteoarchaeol. 23 (4), 421–431.
Guatelli-Steinberg, D., Larsen, C.S., Hutchinson, D.L., 2004. Prevalence and the duration of linear enamel hypoplasia: A comparative study of Neandertals and Inuit foragers. J. Hum. Evol. 47 (1–2), 65–84.
Guatelli-Steinberg, D., 2004. Analysis and significance of linear enamel hypoplasia in Plio-Pleistocene hominins. Am. J. Phys. Anthropol. 123 (3), 199–215.
Guatelli-Steinberg, D., 2003. Macroscopic and microscopic analyses of linear enamel hypoplasia in Plio-Pleistocene South African hominins with respect to aspects of enamel development and morphology. Am. J. Phys. Anthropol. 120 (4), 309–322.
Guy, F., Lazzari, V., Gilissen, E., Thiery, G., 2015. To what extent is primate second molar enamel occlusal morphology shaped by the enamel-dentine junction? PLoS One 10 (9), e0138802.
Henrion, J., Hublin, J.J., Maureille, B., 2023. New Neanderthal remains from the Châtelperronian-attributed layer X of the Grotte du Renne (Arcy-sur-Cure, France). J. Hum. Evol. 181, 103402.
Herries, A.I.R., Martin, J.M., Leece, A.B., Adams, J.W., Boschian, G., Joannes-Boyau, R., Edwards, T.R., Mallett, T., Massey, J., Mursewski, A., Neubauer, S., Pickering, R., Strait, D.S., Armstrong, B.J., Baker, S., Caruana, M.V., Denham, T., Hellstrom, J., Moggi-cecchi, J., Mokobane, S., Penzo-Kajewski, P., Rovinsky, D.S., Schwartz, G.T., Stammers, R.C., Wilson, C., Woodhead, J., Menter, C., 2020. Contemporaneity of *Australopithecus*, *Paranthropus*, and early *Homo erectus* in South Africa. Science 368 (6486), eaaw7293.
Herries, A.I.R., 2022. Chronology of the Hominin Sites of Southern Africa. Oxford Research Encyclopedias, Anthropology, Oxford. https://doi.org/10.1093/acrefore/9780190854584.013.57.
Hillson, S.W., 1992. Dental enamel growth, perikymata and hypoplasia in ancient tooth crowns. J. R. Soc. Med. 85 (8), 460–466.
Hillson, S., Bond, S., 1997. Relationship of enamel hypoplasia to the pattern of tooth crown growth: A discussion. Am. J. Phys. Anthropol. 104 (1), 89–103.
Howell, F.C., 1969. Remains of Hominidae from Pliocene/Pleistocene formations in the lower Omo basin, Ethiopia. Nature 223 (5212), 1234–1239.
Howell, F.C., Coppens, Y., 1973. Deciduous teeth of Hominidae from the Pliocene/Pleistocene of the lower Omo basin, Ethiopia. J. Hum. Evol. 2 (6), 461–472.
Howell, F.C., Haesaerts, P., de Heinzelin, J., 1987. Depositional environments, archeological occurrences and hominids from Members E and F of the Shungura Formation (Omo basin, Ethiopia). J. Hum. Evol. 16 (7–8), 665–700.
Hlusko, L.J., 2004. Protostylid variation in *Australopithecus*. J. Hum. Evol. 46 (5), 579–594.
Hlusko, L.J., Carlson, J.P., Chaplin, G., Elias, S.A., Hoffecker, J.F., Huffman, M., Jablonski, N.G., Monson, T.A., O'Rourke, D.H., Pilloud, M.A., Scott, G.R., 2018. Environmental selection during the last ice age on the mother-to-infant transmission of vitamin D and fatty acids through breast milk. Proc. Natl. Acad. Sci. 115 (19), E4426–E4432.
Hlusko, L.J., Guy, F., Modesto-Mata, M., de Pinillos, M.M., Brasil, M.F., Towle, I., Thiebaut, A., Boisserie, J.R., 2024. Taxonomic assignments for the 3.4 Ma to 1.1 Ma hominin postcanine teeth from the Usno Formation and the Shungura Formation, Lower Omo Valley, Ethiopia. Paleorxiv Preprint. https://doi.org/10.31233/osf.io/g7kfx.
Hoff, M., Van Grunsven, M.F., Jongebloed, W.L., 1975. Enamel defects associated with tuberous sclerosis: A clinical and scanning-electron-microscope study. Oral Surg. Oral Med. Oral Pathol. 40 (2), 261–269.
Howell, F.C., Coppens, Y., 1974. Inventory of remains of Hominidae from Pliocene/Pleistocene formations of the lower Omo basin, Ethiopia (1967–1972). Am. J. Phys. Anthropol. 40 (1), 1–16.
Howell, F.C., Coppens, Y., 1976. An overview of Hominidae from the Omo succession, Ethiopia. In: Earliest Man and Environments in the Lake Rudolf Basin. University of Chicago Press, Chicago, pp. 522–532.
Huang, H., Ba, Y., Cui, L., Cheng, X., Zhu, J., Zhang, Y., Yan, P., Zhu, C., Kilfoy, B., Zhang, Y., 2008. COL1A2 gene polymorphisms (Pvu II and Rsa I), serum calciotropic hormone levels, and dental fluorosis. Community Dent. Oral Epidemiol. 36 (6), 517–522.
Hunt, K., Vitzthum, V.J., 1986. Dental metric assessment of the Omo fossils: Implications for the phylogenetic position of *Australopithecus africanus*. Am. J. Phys. Anthropol. 71 (2), 141–155.
Infante, P.F., Gillespie, G.M., 1974. An epidemiologic study of linear enamel hypoplasia of deciduous anterior teeth in Guatemalan children. Arch. Oral Biol. 19 (11), 1055–1061.
Ioannou, S., Henneberg, M., Henneberg, R.J., Anson, T., 2015. Diagnosis of mercurial teeth in a possible case of congenital syphilis and tuberculosis in a 19th century child skeleton. J. Anthropol. 2015, 1–11.
Irish, J.D., Black, W., Sealy, J., Ackermann, R.R., 2014. Questions of Khoesan continuity: Dental affinities among the indigenous Holocene peoples of South Africa. Am. J. Phys. Anthropol. 155 (1), 33–44.
Jiang, M., Mu, L., Wang, Y., Yan, W., Jiao, Y., 2015. The relationship between Alu I polymorphisms in the calcitonin receptor gene and fluorosis endemic to Chongqing, China. Med. Princ. Pract. 24 (1), 80–83.
Jolly, C.J., 1993. Species, subspecies, and baboon systematics. In: Kimbel, W.H., Martin, L.B. (Eds.), Species, Species Concepts and Primate Evolution. Advances in Primatology. Springer, Boston, MA. https://doi-org.libproxy.berkeley.edu/10.1007/978-1-4899-3745-2_4.
Kaifu, Y., Kono, R.T., Sutikna, T., Saptomo, E.W., Jatmiko, Due Awe, R., 2015a. Unique dental morphology of *Homo floresiensis* and its evolutionary implications. PLoS One 10 (11), e0141614.
Kaifu, Y., Kono, R.T., Sutikna, T., Saptomo, E.W., Awe, R.D., Baba, H., 2015b. Descriptions of the dental remains of *Homo floresiensis*. Anthropol. Sci. 123 (2), 129–145.
Kierdorf, H., Kierdorf, U., Richards, A., Josephsen, K., 2004. Fluoride-induced alterations of enamel structure: An experimental study in the miniature pig. Anat. Embryol. 207, 463–474.
Kierdorf, U., Kierdorf, H., Sedlacek, F., Fejerskov, O., 1996. Structural changes in fluorosed dental enamel of red deer (*Cervus elaphus* L.) from a region with severe environmental pollution by fluorides. J. Anat. 188 (Pt 1), 183.
Kim, Y.J., Shin, T.J., Hyun, H.K., Lee, S.H., Lee, Z.H., Kim, J.W., 2016. A novel de novo mutation in LAMB 3 causes localized hypoplastic enamel in the molar region. Eur. J. Oral Sci. 124 (4), 403–405.
Küchler, E.C., Dea Bruzamolin, C., Ayumi Omori, M., Costa, M.C., Antunes, L.S., Pecharki, G.D., Trevilatto, P.C., Vieira, A.R., Brancher, J.A., 2018. Polymorphisms in nonamelogenin enamel matrix genes are associated with dental fluorosis. Caries Res 52 (1–2), 1–6.
Lacruz, R.S., Habelitz, S., Wright, J.T., Paine, M.L., 2017. Dental enamel formation and implications for oral health and disease. Physiol. Rev. 97 (3), 939–993.
Lockey, A.L., Alemseged, Z., Hublin, J.J., Skinner, M.M., 2020. Maxillary molar enamel thickness of Plio-Pleistocene hominins. J. Hum. Evol. 142, 102731.

Louail, M., Prat, S., 2018. Readjustment of the standard ASUDAS to encompass dental morphological variations in Plio-Pleistocene hominins. Bull. Mem. Soc. Anthropol. Paris 30, 32–48.
Lovell, N.C., Whyte, I., 1999. Patterns of dental enamel defects at ancient Mendes, Egypt. Am. J. Phys. Anthropol. 110 (1), 69–80.
Lukacs, J.R., 2001a. Enamel hypoplasia in the deciduous teeth of early Miocene catarrhines: Evidence of perinatal physiological stress. J. Hum. Evol. 40 (4), 319–329.
Lukacs, J.R., 2001b. Enamel hypoplasia in the deciduous teeth of great apes: Variation in prevalence and timing of defects. Am. J. Phys. Anthropol. 116, 199–208.
Lumley, H.D., 1972. La grotte de l'Hortus. Études quaternaires, mémoire, (1).
Lumley, Marie-Antoinette de, 1973. Ante-Neanderthals and Neanderthals of the Western European Mediterranean Basin. University of Provence, Aix-en-Provence.
Marchenko, A.V., Nikolishyna, E.V., Ilenko, N.M., Nikolishyn, I.A., Kostyrenko, O.P., Cherniak, V.V., 2024. Morphological features of enamel in fluorosis of different degrees of severity. Rep. Morphol. 30 (2), 53–60.
Martinez-Mier, E.A., Shone, D.B., Buckley, C.M., Ando, M., Lippert, F., Soto-Rojas, A.E., 2016. Relationship between enamel fluorosis severity and fluoride content. J. Dent. 46, 42–46.
Martín-Francés, L., 2015. Revisión y estudio de las manifestaciones paleopatológicas en los homininos del plio-pleistoceno, con especial referencia a algunos fósiles de la Sierra de Atapuerca. dissertation. Universidad de Alcalá, Alacalá.
Martín-Francés, L., de Castro, J.M.B., de Pinillos, M.M., Martinón-Torres, M., Arsuaga, J.L., Bertrand, B., Vialet, A., 2022. Middle Pleistocene hominin teeth from Biache-Saint-Vaast, France. Archaeol. Anthropol. Sci. 14 (11), 215.
Martin, R.M., Hublin, J.J., Gunz, P., Skinner, M.M., 2017. The morphology of the enamel–dentine junction in Neanderthal molars: Gross morphology, non-metric traits, and temporal trends. J. Hum. Evol. 103, 20–44.
Martin, J.M., Leece, A.B., Neubauer, S., Baker, S.E., Mongle, C.S., Boschian, G., Schwartz, G.T., Smith, A.L., Ledogar, J.A., Strait, D.S., Herries, A.I.R., 2021. Drimolen cranium DNH 155 documents microevolution in an early hominin species. Nat. Ecol. Evol. 5, 38–45. https://doi.org/10.1038/s41559-020-01319-6.
Martin, J.M., Leece, A.B., Baker, S.E., Herries, A.I.R., Strait, D.S., 2024. A lineage perspective on hominin taxonomy and evolution. Evol. Anthropol. Issues News Rev. 33 (2), e22018.
Mehta, D.N., Shah, J., Thakkar, B., 2013. Amelogenesis imperfecta: Four case reports. J. Nat. Sci. Biol. Med. 4 (2), 462.
Miszkiewicz, J.J., 2015. Linear enamel hypoplasia and age-at-death at medieval (11th–16th Centuries) St. Gregory's Priory and Cemetery, Canterbury, UK. Int. J. Osteoarchaeol. 25 (1), 79–87.
Moggi-Cecchi, J., Menter, C., Boccone, S., Keyser, A., 2010. Early hominin dental remains from the Plio-Pleistocene site of Drimolen, South Africa. J. Hum. Evol. 58 (5), 374–405.
Molnar, S., Molnar, I.M., 1985. The incidence of enamel hypoplasia among the Krapina Neandertals. Am. Anthropol. 87 (3), 536–549.
Nakayama, N., 2016. The relationship between linear enamel hypoplasia and social status in 18th to 19th century Edo, Japan. Int. J. Osteoarchaeol. 26 (6), 1034–1044.
Ogden, A.R., Pinhasi, R., White, W.J., 2007. Gross enamel hypoplasia in molars from subadults in a 16th-18th century London graveyard. Am. J. Phys. Anthropol. 133, 957–966.
Ogilvie, M.D., Curran, B.K., Trinkaus, E., 1989. Incidence and patterning of dental enamel hypoplasia among the Neandertals. Am. J. Phys. Anthropol. 79 (1), 25–41.
O'Hara, M.C., 2021. Features of catarrhine posterior dental crowns associated with durophagy: Implications for fossil hominins. Doctoral dissertation. The Ohio State University, Columbus.
O'Hara, M.C., McGraw, W.S., Guatelli-Steinberg, D., 2023. Some orangutans acquire enamel defects at regular intervals, but not according to seasonal cycles. Am. J. Phys. Anthropol. 180 (3), 519–533.
Paine, O.C., Koppa, A., Henry, A.G., Leichliter, J.N., Codron, D., Lambert, J.E., Codron, J., Sponheimer, M., 2019. Seasonal and habitat effects on the nutritional properties of savanna vegetation: Potential implications for early hominin dietary ecology. J. Hum. Evol. 133, 99–107.
Paulson, R., Schroeder, K., Zacherl, W., Sciulli, P., 1984. Scanning electron microscopy of cusp-tip pits in developing and mature human dentitions. Arch. Oral Biol. 29 (2), 117–125.
Pavličev, M., Cheverud, J.M., 2015. Constraints evolve: Context dependency of gene effects allows evolution of pleiotropy. Annu. Rev. Ecol. Evol. Systemat. 46, 413–434.
Pindborg, J.J., 1970. Pathology of the Dental Hard Tissues. W.B. Saunders, Philadelphia.
Poulter, J.A., Brookes, S.J., Shore, R.C., Smith, C.E., Abi Farraj, L., Kirkham, J., Inglehearn, C.F., Mighell, A.J., 2014. A missense mutation in ITGB6 causes pitted hypomineralized amelogenesis imperfecta. Hum. Mol. Genet. 23 (8), 2189–2197.
Puech, P.F., Albertini, H., 1981. Enamel pits of the Lazaret man. J. Hum. Evol. 10 (6), 449–452.
Purvis, R.J., MacKay, G.S., Cockburn, F., Barrie, W.M., Wilkinson, E.M., Belton, N.R., Forfar, J.O., 1973. Enamel hypoplasia of the teeth associated with neonatal tetany: A manifestation of maternal vitamin-D deficiency. Lancet 302 (7833), 811–814.
Radu, C., Soficaru, A.D., 2016. Dental developmental defects in a subadult from 16th–19th centuries Bucharest, Romania. Int. J. Paleopathol. 15, 33–38.
Robinson, J.T., 1956. The dentition of the Australopithecinae: Maxillary molars. Transvaal Mus. Mem. 9 (1), 81–100.
Ruben, J.L., Roeters, F.J.M., Truin, G.J., Loomans, B.A., Huysmans, M.C.D., 2019. Cup-shaped tooth wear defects: More than erosive challenges? Caries Res. 53 (4), 467–474.
Samuel, S.R., Lai, C.W.M., Khan, M.M., Mathew, M.G., Kramer, M.S., Hsu, C.Y., 2023. Gestational serum retinol deficiency is associated with enamel hypoplasia. J. Dent. Res. 102 (13), 1417–1424.
Schindelin, J., Rueden, C.T., Hiner, M.C., Eliceiri, K.W., 2015. The ImageJ ecosystem: An open platform for biomedical image analysis. Mol. Reprod. Dev. 82 (7–8), 518–529.
Schultz, M., Carli-Thiele, P., Schmidt-Schultzf, T.H., Kierdorf, U., Kierdorf, H., Teegen, W.R., Kreutz, K., 1998. Enamel hypoplasias in archaeological skeletal remains. In: Dental Anthropology: Fundamentals, Limits and Prospects. Springer Vienna, Vienna, pp. 293–311.
Schulze, C., 1970. Developmental abnormalities of the teeth and jaws. In: Gorlin, R.J., Goldman, H.M. (Eds.), Thoma's Oral Pathology, 6th ed. The CV Mosby Co, St. Louis, pp. 96–183.
Seow, W.K., 1993. Clinical diagnosis and management strategies of amelogenesis imperfecta variants. Pediatr. Dent. 15 (6), 384–393.
Seow, W.K., Brown, J.P., Tudehope, D.A., O'Callaghan, M., 1984. Dental defects in the deciduous dentition of premature infants with low birth weight and neonatal rickets. Pediatr. Dent. 6 (2), 88–92.
Seow, W.K., 1990. Enamel hypoplasia in the primary dentition: A review. J. Dent. Child. 58, 441–452.
Skinner, M., 1996. Developmental stress in immature hominines from Late Pleistocene Eurasia: Evidence from enamel hypoplasia. J. Archaeol. Sci. 23 (6), 833–852.
Skinner, M.F., 2023. Meaningful measures of enamel hypoplasia: Prevalence and comparative intensity of developmental stress. Am. J. Phys. Anthropol. 180 (4), 761–767.
Skinner, M.F., Newell, E.A., 2003. Localized hypoplasia of the primary canine in bonobos, orangutans, and gibbons. Am. J. Phys. Anthropol. 120 (1), 61–72.
Skinner, M.M., Alemseged, Z., Gaunitz, C., Hublin, J.J., 2015. Enamel thickness trends in Plio-Pleistocene hominin mandibular molars. J. Hum. Evol. 85, 35–45.
Skinner, M.M., Leakey, M.G., Leakey, L.N., Manthi, F.K., Spoor, F., 2020. Hominin dental remains from the Pliocene localities at Lomekwi, Kenya (1982–2009). J. Hum. Evol. 145, 102820.
Smith, T.M., Olejniczak, A.J., Kupczik, K., Lazzari, V., Vos, J.D., Kullmer, O., Schrenk, F., Hublin, J.J., Jacob, T., Tafforeau, P., 2009. Taxonomic assessment of the Trinil molars using non-destructive 3D structural and development analysis. PaleoAnthropology 117–129.
Smith, C.E., Poulter, J.A., Antanaviciute, A., Kirkham, J., Brookes, S.J., Inglehearn, C.F., Mighell, A.J., 2017. Amelogenesis imperfecta; genes, proteins, and pathways. Front. Physiol. 8, 435.
Smith, T.M., Tafforeau, P., Le Cabec, A., Bonnin, A., Houssaye, A., Pouech, J., …, Menter, C.G., 2015. Dental ontogeny in Pliocene and early Pleistocene hominins. PLoS One 10 (2), e0118118.
Sognnaes, R.F., 1956. Histologic evidence of developmental lesions in teeth originating from Paleolithic, prehistoric, and ancient man. Am. J. Pathol. 32 (3), 547.
Stimmler, L., Snodgrass, G.J.A.I., Jaffe, E., 1973. Dental defects associated with neonatal symptomatic hypocalcaemia. Arch. Dis. Child. 48 (3), 217.
Sundell, S., Koch, G., 1985. Hereditary amelogenesis imperfecta. I. Epidemiology and clinical classification in a Swedish child population. Swed. Dent. J. 9 (4), 157–169.
Suwa, G.E.N., Asfaw, B., Haile-Selassie, Y., White, T.I.M., Katoh, S., WoldeGabriel, G., …, Beyene, Y., 2007. Early pleistocene Homo erectus fossils from konso, southern Ethiopia. Anthropol. Sci. 115 (2), 133–151.
Suwa, G., White, T.D., Howell, F.C., 1996. Mandibular postcanine dentition from the Shungura Formation, Ethiopia: Crown morphology, taxonomic allocations, and Plio-Pleistocene hominid evolution. Am. J. Phys. Anthropol. 101 (2), 247–282.
Ten Cate, A., 1994. Structure of the oral tissues. In: Ten Cate, A.R. (Ed.), Oral Histology: Development, Structure and Function. Mosby, St. Louis, pp. 45–57.
Thackeray, J.F., Kirschvink, J.L., Raub, T.D., 2002. Palaeomagnetic analyses of calcified deposits from the Plio-Pleistocene hominid site of Kromdraai, South Africa. S. Afr. J. Sci. 98, 537–540.
Tobias, P.V., 1967. The Cranium and Maxillary Dentition of *Australopithecus* (*Zinjanthropus*) *Boisei*. Cambridge University Press, Cambridge.
Towle, I., Irish, J.D., 2019. A probable genetic origin for pitting enamel hypoplasia on the molars of *Paranthropus robustus*. J. Hum. Evol. 129, 54–61.
Towle, I., Irish, J.D., 2020. Recording and interpreting enamel hypoplasia in samples from archaeological and palaeoanthropological contexts. J. Archaeol. Sci. 114, 105077.
Towle, I., Irish, J.D., Groote, I.D., Fernée, C., Loch, C., 2021. Dental caries in South African fossil hominins. South Afr. J. Sci. 117 (3–4), 1–8.
Towle, I., Loch, C., 2024. Variation in enamel prism size in primate molars. Arch. Oral Biol., 105895
Towle, I.E., 2017. Dental pathology, wear and developmental defects in South African hominins. Ph.D. Dissertation thesis, Liverpool John Moores University.
Towle, I., Dove, E.R., Irish, J.D., De Groote, I., 2017. Severe plane-form enamel hypoplasia in a dentition from Roman Britain. Dental Anthropol. 30, 16–24.
Towle, I., Irish, J.D., De Groote, I., 2018. Amelogenesis imperfecta in the dentition of a wild chimpanzee. J. Med. Primatol. 47 (2), 117–119.

Towle, I., Loch, C., Martínez de Pinillos, M., Modesto-Mata, M., Hlusko, L.J., 2023. Severe enamel defects in wild Japanese macaques. Int. J. Zool. 2024 (1), 8445492. https://doi.org/10.1155/2024/8445492.

Towle, I., O'Hara, M., Leece, A., Herries, A.I.R., Adjei, A., Guatelli-Steinberg, D., Martínez de Pinillos, M., Modesto-Mata, M., Thiebaut, A., Hernando, R., Irish, J.D., Guy, F., Boisserie, J.-R., Hlusko, L., 2025. Uniform, circular and shallow (UCS) enamel pitting in hominins: Prevalence, morphological associations, and potential taxonomic significance. DRYAD. https://doi.org/10.5061/dryad.69p8cz9f9.

Trinkaus, E., 1987. The Upper Pleistocene Human Molar From Me'arat Shovakh (Mugharet esh-Shubbabiq), Israel. Paleorient, Paris, pp. 95–100.

White, T.D., 1978. Early hominid enamel hypoplasia. Am. J. Phys. Anthropol. 49 (1), 79–83.

White, T.D., Lovejoy, C.O., Asfaw, B., Carlson, J.P., Suwa, G., 2015. Neither chimpanzee nor human, *Ardipithecus* reveals the surprising ancestry of both. Proc. Natl. Acad. Sci. 112 (16), 4877–4884.

Witkop Jr., C.J., 1988. Amelogenesis imperfecta, dentinogenesis imperfecta and dentin dysplasia revisited: Problems in classification. J. Oral Pathol. 17, 547–553.

Witkop Jr., C.J., Sauk Jr., J.J., 1976. Heritable defects of enamel. In: Prescott, G., Stewart, R. (Eds.), Oral Facial Genetics. CV Mosby Company, St Louis, pp. 151–226.

Witzel, C., Kierdorf, U., Dobney, K., Ervynck, A., Vanpoucke, S., Kierdorf, H., 2006. Reconstructing impairment of secretory ameloblast function in porcine teeth by analysis of morphological alterations in dental enamel. J. Anat. 209 (1), 93–110.

Wood, B.A., Abbott, S.A., Graham, S.H., 1983. Analysis of the dental morphology of Plio-Pleistocene hominids. II. Mandibular molars–study of cusp areas, fissure pattern and cross sectional shape of the crown. J. Anat. 137 (Pt 2), 287.

Wood, B., Leakey, M., 2011. The Omo-Turkana Basin fossil hominins and their contribution to our understanding of human evolution in Africa. Evol. Anthropol. 20 (6), 264–292.

Wood, B.A., Xu, Q., 1991. Variation in the Lufeng dental remains. J. Hum. Evol. 20 (4), 291–311.

Wright, J.T., 1985. Analysis of a kindred with amelogenesis imperfecta. J. Oral Pathol. Med. 14 (5), 366–374.

Wright, J.T., Fine, J.D., Johnson, L., 1993. Hereditary epidermolysis bullosa: Oral manifestations and dental management. Pediatr. Dent. 15, 242–248.

Wu, X., 2024. Research progress on human fossils from the Xujiayao site in late Middle Pleistocene. Acta Anthropol. Sin. 43 (1), 5.

Xing, S., Guatelli-Steinberg, D., O'Hara, M., Li, J., Wei, P., Liu, W., Wu, X., 2016. Micro-CT imaging and analysis of enamel defects on the early late Pleistocene Xujiayao Juvenile. Int. J. Osteoarchaeol. 26 (6), 935–946.

Xing, S., Tafforeau, P., O'hara, M., Modesto-Mata, M., Martín-Francés, L., Martinón-Torres, M., Zhang, L., Schepartz, L.A., Bermúdez de Castro, J.M., Guatelli-Steinberg, D., 2019. First systematic assessment of dental growth and development in an archaic hominin (genus, *Homo*) from East Asia. Sci. Adv. 5 (1), eaau0930.

Zanolli, C., Dean, M.C., Assefa, Y., Bayle, P., Braga, J., Condemi, S., Endalamaw, M.E., Redae, B.E., Macchiarelli, R., 2017. Structural organization and tooth development in a Homo aff. erectus juvenile mandible from the Early Pleistocene site of Garba IV at Melka Kunture, Ethiopian highlands. Am. J. Phys. Anthropol. 162 (3), 533–549.

Zilberman, U., Smith, P., Piperno, M., Condemi, S., 2004. Evidence of amelogenesis imperfecta in an early African *Homo erectus*. J. Hum. Evol. 46 (6), 647–653.